Rheinische Friedrich-Wilhelms-Universität Bonn

Geographisches Institut

Dynamics of greenhouse gas emissions and nitrogen availability as influenced by biochar particles during composting

Masterarbeit

im Rahmen des Masterstudiengangs

Geographie

zur Erlangung des akademischen Grades

Master of Science (M.Sc.)

vorgelegt von Franziska Louise Busch

vorgelegt am 01.08.2023

Betreut durch

Prof. Dr. Julian Klaus

Dr. Otávio dos Anjos Leal

Erklärung

Ich versichere, dass ich die Arbeit selbstständig verfasst habe, dass ich keine anderen Quellen und Hilfsmittel als die angegebenen benutzt und die Stellen der Arbeit, die anderen Werken dem Wortlaut oder dem Sinn nach entnommen sind, in jedem Fall als Entlehnung kenntlich gemacht habe. Das Gleiche gilt auch für beigegebene Tabellen und Abbildungen. Der Textteil der Arbeit (inkl. Leerzeichen und Anmerkungen) umfasst 117.245 Zeichen.

Bonn, den 1.8.2023 Rusl

Ort, Datum Unterschrift der Studierende

Acknowledgements

I would like to thank all my colleagues at Forschungszentrum Jülich for their help, expertise and guidance during this experiment and my learning process. Special thanks go to the lab technicians Franz Leistner, Holger Wissel and Sirgit Kummer, whose useful tips made many steps easier for me. In addition, I would like to thank all the strong assisting hands who helped me mixing the feedstocks on the first day. And to all the people who supported me with the sampling and taught me many new methods. I would also like to thank the companies Burgmühle and Stütgerhof for providing the horse manure and vegetable scraps free of charge.

Abstract

In this study, a 148-day composting of vegetable waste, horse manure and wheat straw was conducted to investigate the greenhouse gas (GHG) emissions and nitrogen (N) dynamics as influenced by the addition of biochar (bc). A special research focus has been placed on the retention of the N-forms by the bc. GHG (CO_2, CH_4, N_2O) were measured with gas chromatography and mineral N of the compost substrate was analyzed with standard methods (0.01 mol L^{-1} $CaCl_2$). In addition, N retained by bc particles was analyzed by a three-stage extraction procedure and bc particles were also analyzed by ^{13}C NMR spectroscopy. These methods provided a comprehensive insight into the temporal dynamics of GHG emissions, the amount and availability of N retained by bc particles, and the change in chemical groups of bc during composting with bc amendment. The addition of bc (15%) did not significantly reduce or increase GHG emissions compared to the control (ctrl) compost. Cumulative emissions averaged at 4016 (ctrl) and 3706 (bc) g CO_2-C m^{-2}, 2171 (ctrl) and 3332 (bc) mg CH_4-C m^{-2} and 715 (ctrl) and 562.8 (bc) mg N_2O-N m^{-2}. The concentrations of NH_4^+–N, NO_3^-–N, NO_2^-–N did not differ significantly between the treatments, but significantly higher (54%) total amounts of NO_3^-–N (g $pile^{-1}$) were measured for the whole compost pile in the bc treatment, indicating lower NO_3^{-1} losses throughout the composting. The retention of N forms by bc particles was not reflected in significantly lower N_2O emissions. However, N forms were effectively retained in varying degrees of strength by the bc particles. The NH_4^+–N concentrations that could be extracted from the bc particles decreased during the composting process. The percentage distribution shows a clear transition from predominantly plant-available (55%) at the beginning of composting to predominantly tightly bound (75%) NH_4^+–N in the final compost. At the end of the composting process, the extractable NO_3^-–N concentration from bc particles was 164 mg kg^{-1} (easily extractable), 80 mg kg^{-1} (not available) and 194 mg kg^{-1} (strongly retained). Until the last day of composting, these concentrations increased continuously with a distribution towards rather strongly bound NO_3^-–N. It can be concluded that the addition of bc tended to protect against N losses.

Zusammenfassung

Über einen Zeitraum von 148 Tagen wurden Gemüseabfälle, Pferdemist und Weizenstroh unter Zugabe von Pflanzenkohle (Biochar) in Holzkompostern kompostiert. Dabei wurden die Treibhausgasemissionen (THG) und die Stickstoffdynamik im Kompost unter dem Einfluss von Pflanzenkohle (Biochar) untersucht. Der Schwerpunkt der Untersuchungen lag darauf, in welchen Formen und mit welcher Verfügbarkeit N durch die Pflanzenkohle zurückgehalten wird. Die THG Emissionen (CO_2, CH_4, N_2O) wurden mittels Gaschromatographie gemessen und der mineralische N-Gehalt des Kompostsubstrats wurde mit Standardmethoden (0.01 mol L^{-1} $CaCl_2$) analysiert. In einem dreistufigen Extraktionsverfahren wurden die Formen und die Verfügbarkeit des in der Pflanzenkohle zurückgehaltenen N analysiert. Die Veränderung der chemische Zusammensetzung nach der Kompostierung wurde mittels ^{13}C-NMR-Spektroskopie untersucht. Diese Methoden ermöglichten eine umfassende Analyse der THG-Dynamik, der Menge und Verfügbarkeit des zurückgehaltenen N sowie der Veränderung der chemischen Gruppen der Pflanzenkohle während der Kompostierung mit Pflanzenkohlezusatz. Die Zugabe von 15 % Pflanzenkohle führte im Vergleich zum Kontrollkompost weder zu einer signifikanten Reduktion noch zu einer Erhöhung der THG-Emissionen. Die kumulierten Emissionen betrugen im Mittel 4016 (Kontrolle) bzw. 3706 (Biochar) g CO_2-C m^{-2}, 2171 (Kontrolle) bzw. 3332 (Biochar) mg CH_4-C m^{-2} und 715 (Kontrolle) bzw. 563 (Biochar) mg N_2O-N m^{-2} ohne signifikante Unterschiede zwischen den beiden Gruppen. Die Konzentrationen von NH_4^+-N, NO_3^--N, NO_2^--N unterschieden sich nicht signifikant zwischen den Behandlungen, jedoch wurden signifikant höhere Gesamtmengen (54 %) an NO_3^--N (g $pile^{-1}$) im gesamten Komposthaufen durch die Zugabe von Pflanzenkohle gemessen. Der Rückhalt von Stickstoffformen durch die Pflanzenkohle spiegelt sich nicht in signifikant geringeren N_2O Emissionen wieder. Die prozentuale Verteilung des aus der Pflanzenkohle extrahierten NH_4^+-N zeigt eine Verschiebung von überwiegend leicht extrahierbar (55 %) zu Beginn zu überwiegend stark gebunden (75 %) am Ende der Kompostierung. Der NO_3^--N Gehalt in der Pflanzenkohle hat während der Kompostierung zugenommen. Am Ende wurden NO_3^--N Konzentrationen von 164 mg kg^{-1} (leicht extrahierbar), 80 mg kg^{-1} (nicht verfügbar) und 194 mg kg^{-1} (stark zurückgehalten) von den Pflanzenkohlepartikeln extrahiert. Es zeigt sich eine Verteilung hin zu eher stark gebundenem NO_3^--N, woraus geschlossen werden kann, dass die Zugabe von Pflanzenkohle tendenziell vor N-Verlusten durch Auswaschung schützt.

Contents

List of figures

List of tables

List of abbreviations

^{13}C-NMR	^{13}C-nucler magnetic resonance spectroscopy
bc	biochar
BET	Specific surface area according to Brunauer-Emmett-Teller equation
C	Carbon
Ca	Calcium
CH_4	Methane
C/N-ratio	Carbon-to-nitrogen-ratio
CO_2	Carbon dioxide
ctrl	control
dw	Dry weight
EBC	European Biochar Certificate
EC	Electrical conductivity
FAO	Food and Agriculture Organization of the United Nations
GHG	Greenhouse gas
GI	Germination index
GWP	Global warming potential
HM	Horse manure
IBG-3	Institute of Bio- and Geosciences-Agrosphere
K	Potassium
K_{av}	Plant-available potassium
MC	Moisture content
N	Nitrogen
NH_3	Ammonia
NH_4^+	Ammonium
NH_4^+–N	Nitrogen in the form of ammonium
N_{min}	Mineral nitrogen
NO	Nitric oxide
NO_2^-	Nitrite
NO_2^-–N	Nitrogen in the form of nitrite
NO_3^-	Nitrate
NO_3^-–N	Nitrogen in the form of nitrate
N_2O	Nitrous oxide
O_2	Oxygen
OM	Organic matter
OriBc	original biochar
P	Phosphorus
Pav	Plant-available phosphorus
SE	Standard error
TK	Total potassium
TN	Total nitrogen
TOC	Total organic carbon
TOM	Total organic matter
TP	Total phosphorus
VDLUFA	Association of German Agricultural Analytic and Research Institutes
VS	Vegetable scraps
WS	Wheat straw

1. Introduction

1.1 Research background

Agricultural practices contribute significantly to global warming due to their high proportion of anthropogenic greenhouse gas (GHG) emissions, but also result in removals from the atmosphere. About 23% of anthropogenic GHG emissions, namely carbon dioxide (CO_2), methane (CH_4) and nitrous oxide (N_2O), are caused by agriculture, forestry and other land uses (Jia et al., 2019). Livestock production, due to enteric fermentation and storage of manure, synthetic fertilizers and biomass combustion are considered to be the sectors with the highest GHG emissions within agriculture (Fróna et al., 2019). Agricultural intensification has also led to major anthropogenic disturbances of the natural nitrogen (N) cycle in recent decades (Bouwman et al., 2013; Canadell et al., 2021). A potential imbalance between N supply and N demand by crops can lead to increased N losses from the soils (Ammonia (NH_3) volatilization, N_2O and nitric oxide (NO) emissions and nitrate (NO_3^-) leaching) with adverse environmental impacts (Fowler et al., 2013). The deposition of NH_3 to soils can damage natural ecosystems through eutrophication and acidification, N_2O is a long-lived GHG that accumulates in the atmosphere, NO is important in tropospheric ozone chemistry, and leaching of NO_3^- into water bodies can lead to eutrophication and may be problematic for drinking water standards (Bouwman et al., 2013). The most recent Special Report on Climate Change and Land of the Intergovernmental Panel on Climate Change (IPCC) concluded that agriculture is the main anthropogenic source of N_2O, mainly due to the application of N to soils (Jia et al., 2019; Canadell et al., 2021). According to this report, 50% of the N applied to agricultural land is not taken up by crops due to the aforementioned lack of synchronization between N supply and demand (Jia et al., 2019). It is therefore important to find sustainable solutions and land management practices that ensure efficient N supply to crops and reduce N losses and GHG emissions.

The use of bc in agriculture has been shown to improve soil biochemical and physical parameters, resulting in reduced GHG emissions, less nutrient leaching and improved soil fertility (Cayuela et al., 2014; Liu et al., 2018; Borchard et al., 2019; Lehmann et al., 2021; Schmidt et al., 2021). Biochar is defined as a carbon (C) rich material produced by the thermal treatment (pyrolysis or gasification) of biomass at high temperatures in the absence or limited presence of oxygen (Fischer & Glaser, 2012; Lehmann & Joseph, 2015). Due to its favourable physicochemical properties, many studies investigate how bc improves soil properties and plant nutrition.

The agro-ecological potential of bc in soil science is also addressed in this study. The experiment was carried out at the Institute of Bio- and Geosciences-Agrosphere (IBG-3) at the Forschungszentrum Jülich (FZJ) (North Rhine-Westphalia, Germany) as part of a research project investigating optimized and more efficient use of N when applying mineral fertilizers to nutrient-poor soils. In this context, the application of co-composted bc is intended to reduce the use of N fertilizers and to regulate a possible N surplus. The aim of this Master's thesis is to characterize the co-composting process of the bc with regard to compost nutrient availability and the GHG emissions dynamics. Particularly, emphasis is given to retention of mineral Nitrogen (N_{min}) forms in bc particles during composting.

In a broader context, the results of this study have potential relevance to nutrient-poor or degraded soils worldwide, such as in post-mining areas, where the original soil and underlying overburden are removed. As a result, anthropogenic soils in these areas are characterized by low organic matter content, poor soil structure and low fertility, with the need for recultivation to support future agricultural use (Schmid et al., 2020). This is particularly the case in areas near Jülich due to its location in the Rhenish lignite mining region. It is important to address these soil challenges and exploit the potential benefits of co-composting bc for efficient fertilization of such soils.
The presence of numerous horse farms in the region, which produce large quantities of manure, also presents an opportunity for sustainable nutrient recycling. As manure is both cheap and nutrient-rich, its efficient treatment, such as composting, can play a key role in increasing soil fertility and nutrient availability. This aspect fits well with the overall aim of the thesis, which is to gain a better understanding of how co-composting of bc can contribute to sustainable agricultural practices in terms of N use efficiency.

1.2 State of the Art

1.2.1 Composting process

Under aerobic conditions, a large variety of microorganisms decompose organic material from plants, food waste, manure or sludge (Rynk et al., 1992; Fischer & Glaser, 2012). Under controlled conditions, this biological process is called composting and the end product is a stable, humus-like substrate that should be free of pathogens and viable seeds (Bernal et al., 2009). Compost can be used as an organic fertilizer to improve soil structure and provide nutrients to plants (Rynk et al., 1992; Román et al., 2015). It has the potential to convert organic waste into inputs for further agricultural production, with benefits including manure management, nutrient recycling, reduced risk of pollution, pathogen destruction and ecological sanitation of residues (Rynk et al., 1992; Román et al., 2015; Castro-Herrera et al., 2023).

In order to obtain a high-quality product that is not harmful to plants, the composting process should go through several phases, including a thermophilic (hot) phase. At the end of the process, final requirements should be fulfilled to avoid phytotoxicity or excess N, which can be harmful to plants or the environment (Bernal et al., 2009). Thermophilic composting is characterized by four phases and the duration of each phase depends on the parameters of the initial feedstock, moisture content (MC), aeration conditions and microbial populations in the compost pile (Fischer & Glaser, 2012).

The decomposition of OM (Organic matter) by micro-organisms using O_2 starts immediately after the raw materials are mixed. At the beginning of composting, the temperature in the compost pile is similar to the ambient temperature. During this phase, labile organic compounds such as sugars, amino acids and proteins present in the starting materials are rapidly degraded by fungi, actinomycetes and bacteria that prefer mesophilic temperatures (Bernal et al., 2009; Fischer & Glaser, 2012). This mineralization and metabolism by microorganisms result in CO_2 and NH_3 emission, organic acids and heat (Bernal et al., 2009). The temperatures inside the compost piles rise rapidly as the heat accumulates. This initial phase, which lasts

only a few days and in which temperatures are still <45°C, is called mesophilic phase I (Rynk et al., 1992).

The next phase is called thermophilic, and begins when temperatures rise above 45°C and thermophilic microorganisms such as actinomycetes or bacillius degrade fats, cellulose, hemicellulose and some lignin (Bernal et al., 2009; Fischer & Glaser, 2012). In this phase, also pathogens, weeds or contaminants of faecal origin are destroyed by the high temperatures (>55°C), thus sanitising the raw material (Bernal et al., 2009; Román et al., 2015; Castro-Herrera et al., 2021). In this very active phase of composting, the rate of decomposition of OM is very high. As a result, the organic C content and consequently the C:N (carbon-to-nitrogen) ratio decreases quickly. There is also a large mass loss due to OM decomposition and the weight of the pile is considerably reduced. The high temperatures are maintained for several days or weeks, depending on the initial material and composting conditions (Rynk et al., 1992).

As the sources of available and labile C decrease, the rate of decomposition of the OM and the pile temperatures gradually decrease (Bernal et al., 2009). When temperatures in the compost pile fall below 45°C, the mesophilic phase II begins. This third phase of composting is also known as the cooling phase (Fischer & Glaser, 2012). During this phase, the compost pile is again actively colonized by mesophilic microorganisms that degrade the remaining and more complex lignin and cellulose compounds (Bernal et al., 2009).

As compost temperatures continue to fall and reach ambient temperatures, the maturation phase is initiated (Rynk et al., 1992). In this final phase, the quality of the compost increases as stabilization and humification of the OM occurs, producing a final mature and stable product with humic characteristics (Bernal et al., 2009, Antunes et al., 2019). Important parameters of maturity and stability according to Bernal et al. (2009) are summarized in Table 1.

Table 1 *Selection of compost parameters that indicate compost maturity and stability according to Bernal et al. (2009).*

Parameter	Value
pH	stable, around neutral
C:N	<20, preferable <12
NH_4^+–N (g kg^{-1})	<0.4
NH_4^+–N:NO_3^-–N	<0.16
CO_2 production rate (mg CO_2 kg^{-1} h^{-1})	<120
GI (%)	>50
Temperature (°C)	constant and around ambient air

During the composting process, CO_2 is released through the respiration of microorganisms and therefore varies with the microbial activity throughout the different phases. At the beginning of the composting high CO_2 emissions occur as a result of the mineralization and metabolism of simple organic C components by microorganisms during the aerobic decomposition (Bernal et al., 2009; Sánchez et al., 2015). Improved aeration by regularly mixing of the piles stimulates the microbial activity and accelerates the composting process, contributing to increased CO_2 emissions after pile turning (Ahn et al., 2011). Due to reduced microbial respiration and the

stabilization of OM, CO_2 emissions get lower towards the end of mesophilic phase II and throughout the maturation phase (Bernal et al., 2009).

Anaerobic decomposition of organic compounds by methanogenic organisms produces CH_4 in a compost (Sonoki et al., 2013; Sánchez et al., 2015). Normally, large amounts of CH_4 should not be produced in well-managed compost, but anaerobic microsites can occasionally develop in piles and cause CH_4 emissions (Rynk et al., 1992; Beck-Friis et al., 2000). In compost, CH_4 should only be produced at high temperatures, which induces the enrichment of anaerobic microorganisms such as methanogens (Jäckel et al., 2005). Due to the high oxygen consumption of microbial degradation of readily available organic compounds and the stimulation of microbial growth, O_2 levels can be depleted and anaerobic patches can develop (Sánchez et al., 2015). As a result, the majority of the CH_4 emissions are measured during the first few weeks of the composting process (Beck-Friis et al., 2000).

As OM decomposes, the N contained in the organic compounds is first released as Ammonium (NH_4^+) (Rynk et al., 1992). Subsequently, NH_4^+ content in the compost decreases which can be attributed to various processes, including nitrification, microbial immobilization, losses by leaching or volatilization (Bernal et al., 2009). In a neutral to alkaline pH range, NH_4^+ begins to dissociate into NH_3, which can be lost due to volatilization (Amelung et al., 2018). The thermophilic phase, where the maximum of OM is degradation rate is reached and the NH_4^+ concentrations are high, favours NH_3 volatilization (Sánchez-Monedero et al., 2001). Also the high pH values and increasing temperatures foster this process (Bernal et al., 2009). Nitrification, when NH_4^+ is converted to NO_3^-, begins when temperatures drop below 45°C (Sánchez-Monedero et al., 2001; Sánchez et al., 2015). This conversion process involves the oxidation of NH_4^+ by nitrifying bacteria and archaea, resulting in the formation of N_2O, nitrite (NO_2^-) and NO_3^- (Amelung et al., 2018). Nitrification hardly occurs in the thermophilic phase, as the high temperatures inhibit the function of nitrifying organisms (Sánchez-Monedero et al., 2001; Sánchez et al., 2015). The intensity of the process depends on the available amount of NH_4^+. By increasing the pile aeration through turning, nitrification rates are increased, resulting in higher N_2O emissions (Ahn et al., 2011). N_2O is also an intermediate product of microbial denitrification and can occur as a result of the of anaerobic microsites within the compost material (Bernal et al., 2009).

1.2.2 Benefits of biochar

The use of bc as an agricultural soil amendment has been shown to have a positive effect on soil fertility and crop yield (Abbruzzini et al., 2019; Schmidt et al., 2021). Biochar can have favourable physical-chemical properties, such as large surface area, numerous pores, abundant functional groups (particularly if produced from non-woody feedstocks during low temperature pyrolysis, and after artificial or natural aging), and a high water holding capacity (Glaser et al., 2000; Schmidt et al., 2021). Due to the change in soil physical properties and the interaction with the soil biota, nutrient dynamics can be altered when bc is applied to soils, possibly resulting in reduced nutrient leaching, mitigation of GHG emissions and enhanced C sequestration (Borchard et al., 2014; Lehmann et al., 2021). The addition of bc to soils has been shown to regulate the soil N cycle through biological N_2 fixation, improved plant uptake, reduced soil N_2O emissions and reduced NO_3^- leaching (Liu et al., 2018; Schmidt et al., 2021).

However, the introduction of an alkaline substrate can also increase NH_3 volatilization by changing the pH conditions (Liu et al., 2018).

In the recent years, many studies have also investigated the possible effects of bc as an additive in organic waste composting (Sánchez-Monedero et al., 2018; Schmidt et al., 2021; Yin et al., 2021; Nguyen et al., 2022). In this context, the conditions of the compost pile can favour the interaction between OM, microbial biomass and nutrient dynamics of the compost material and the bc.

Various properties of the compost substrate can change due to the specific physical structure of the added bc. The bc pores might improve the water retention and aeration, which means that the compost pile does not dry out as quickly and can have better oxygenation (Prost et al., 2013). Due to the abundance of macro- and micropores, the large surface area and a better O_2 supply, bc is a suitable and additional habitat for microorganisms and both microbial population size and diversity increase when composting with bc (Hua et al., 2011; Sun et al., 2016). The improved water and aeration conditions also help to maintain microbial activity for longer (Prost et al., 2013). As the microbial growth is enhanced, also the processes of humification and the degradation of OM are faster and the composting process is accelerated (Zhang & Sun, 2014; Sánchez-García et al., 2015; Awasthi et al., 2017).

The altered activity of the microorganisms and the possible sorption capacity can also change the gas emissions and nutrient dynamics during composting with bc. Several studies report a reduction in N losses, which is reflected in lower N_2O and NH_3 emissions and less NO_3^- leaching (Steiner et al., 2010; Kammann et al., 2015; Hagemann et al., 2017a; Wang et al., 2017; Joseph et al., 2018; Castro-Herrera et al., 2023).

The uptake of NO_3^- by the bc is termed as “nitrate capture” and attenuates NO_3^- leaching from compost (Kammann et al., 2015; Hagemann et al., 2017a). This is controlled by complex binding mechanisms with varying degrees of retention that have been investigated in previous studies. There are several processes that can bind anions to the surface of bc. Nitrate may be trapped within the bc pores or bound to organic coating formed on the bc surface. Initially, nutrient-rich water can enter the pores and, by partially closing the meso- and macropores, can result in NO_3^- being trapped in the micropores (Joseph et al., 2018). Also organo-mineral complexes with dissolved N species can be observed on the co-composted bc particles (Hagemann et al., 2017b; Joseph et al., 2018). Another possible retention mechanism could be due to the formation of weak, unconventional hydrogen bonds in micro- and nanopores of the bc particles, ligand exchange or electrostatic attraction (Conte & Alonzo, 2007; Loganathan et al., 2013; Joseph et al., 2018). Due to the biological and chemical oxidation of bc, it has been shown that composting can induce formation of groups at bc surface (Glaser et al., 2000; Wiedner et al., 2015). These carboxylic and phenolic groups and the sorbed OM on the bc surface can act as sorption sites for NH_4^+ (Prost et al., 2013; Wang et al., 2019). The reduction of N_2O emissions in bc-amended compost depends on different processes and is related to the retention mechanisms described above. The capture of NH_4^+ and NO_3^- by bc particles reduces the pool of inorganic N available to nitrifying and denitrifying bacteria, thereby decreasing N_2O emissions from compost (Kammann et al., 2015; He et al., 2017). As the physical properties of the bc improve aeration conditions in the compost pile, anaerobic patches favourable

to denitrifying microorganisms are reduced and therefore their activity is limited (Li et al., 2016).

The statistical literature review of Firmino and Trémier (2023) on ruling parameters of N losses in bc amended compost found that only 45% of the N loss reduction observed in bc-amended compost could be explained by commonly analyzed bc parameters. Moreover, the authors emphasize the need of further research including analysis of bc chemical structure and N retention strength during composting aiming to add understanding on the complex action of bc as N optimizer in compost.

Most of the recent studies on adding bc to compost have been carried out with pig or chicken manure, and not many results have been published for composting of horse manure with organic waste, which is largely and easily available in the vicinity of FZJ. Additionally, to the best of our knowledge, no study has analyzed concomitantly the temporal dynamics of GHG emissions, the amount and availability of N retained by bc particles and the modifications in bc chemical groups during composting. These important aspects are addressed in this thesis.

1.3 Hypotheses and research questions

To guide this study, the following hypotheses are posed based on the previously presented gap in the current literature and data available on co-composting with bc:

- Biochar retains ammonium and nitrate in available and unavailable forms during composting of organic residues.
- Biochar reduces N loss during composting of horse manure, organic waste and wheat straw.
- During the different phases of the composting process, the nitrification rates and N2O emissions are reduced due to an effective N retention by biochar.
- Biochar functionalization due to co-composting with organic residues may contribute to retain NH4+.

These assumptions were tested through the following research questions:

- How do compost treatments with and without biochar differ in the temporal dynamics of GHG emissions?
- Are the possible lower emissions of N2O reflected in a higher level of retention of N forms by biochar?
- How available are the different forms of N retained by the biochar particles during the composting process?
- How does co-composting affect biochar chemical structure and the formation of carboxylic groups?

2. Material and Methods

2.1 Compost experiment

The compost experiment was conducted at FZJ (North Rhine-Westphalia, Germany). The feedstocks used in the compost experiment were vegetable scraps (VS), horse manure (HM), and wheat straw (WS). The chopped VS (1079.6 kg fresh weight) consisted of a large variety of different vegetables, such as cabbage, apple peel, tomatoes, onions, lemons, lettuce and was provided by Burgmühle (Kerpen, Germany), a supplier to the FZJ's canteen. The HM (503.3 kg fresh weight) was collected with minimal straw supplements from the horse ranch Stütgerhof (Langerwehe, Germany). The VS and HM were maximum two days old. The WS (74.5 kg) was purchased. The VS, HM and WS (totalling 1657.4 kg fresh) were thoroughly mixed by several people using garden forks (Appendix: Figure A.1-3). The characteristics of the initial mixture are described in Table 2.

Table 2 *Attributes of the initial feedstock on composting day 0. Values are reported as mean values ± SE (n=3).*

	Vegetable scraps	Horse manure	Wheat straw
Distribution (%)	43.3	40.9	15.8
kg	1079.6 (wet)	503.3 (wet)	74.5 (dry)
MC (% fresh wt)	91.8	66.8	-
TOC (g kg^{-1})	375.7 ± 1.2	396.1 ± 1.3	423.4 ± 1.3
TN (g kg^{-1})	33.3 ± 0.1	14.6 ± 0.1	5.8 ± 0
C:N	11.3 ± 0.1	27.2 ± 0.3	73.3 ± 0.4
NH_4^+–N (mg kg^{-1})	205.4 ± 8.9	15.2 ± 0.9	-
NO_3^-–N (mg kg^{-1})	0.7 ± 0	6.8 ± 0.2	-
NO_2^-–N (mg kg^{-1})	2.64 ± 0.1	0.5 ± 0	-
P_{av} (mg kg^{-1})	16.9 ± 1.5	476.1 ± 50.2	-
K_{av} (mg kg^{-1})	163.2 ± 12.2	1850.3 ± 278.9	-

To carry out the composting, six wooden boxes (0.85 m x 0.85 m x 1.20 m height) were set up (Appendix: Figure A.4-5). The boxes consisted of piled wooden strips with spaces between the strips to allow air circulation and oxygenation of the compost. As the experiment was conducted outdoors on the FZJ campus, a mesh wire was attached to the outer sides and bottom of the boxes to prevent animals from getting into the piles. The mesh wire served also to retain the residues in the boxes. Each box received 276.2 kg fresh (corresponding to 71.3 kg dry weight(dw)) of the homogeneous mixture of VS (43.3%), HM (40.9%) and WS (15.8%). The initial height of the compost pile was 1.05 m and the bulk density was 480.3 kg m^{-3}.

Out of the six boxes, three of them were randomly selected to receive bc. The control treatments without bc are referred to as "ctrl" and the biochar amended treatments as "bc". The amount of bc added to each of these three boxes was 12.7 kg (10.7 kg dw), resulting in a bc addition to the compost pile of 15% (dw). This bc application rate to compost was chosen since the ideal range usually reported in the literature is 10−20%, and rates >20% may unfavour the

composting process (Sánchez-Monedero et al., 2018). The bc used (AWN Abfallwirtschaft, Buchen) was produced via pyrolysis (680°C) of woody feedstocks of tree and shrub cuttings (Pflanzenkohle aus Baum- und Strauchschnitt). A prerequisite for the selection of the bc was its certification with the European Biochar Certificate (EBC) in order to prevent or reduce possible risks for human health and environment resulting from its production and use. The main characteristics of the bc and the required EBC regulations were analyzed by Eurofins Umwelt Ost GmbH (Bobritzsch-Hilbersdorf, Germany) and are presented in Table 3 and Appendix Table A.1.

Table 3 *Parameters of the biochar delivered from AWN Abfallwirtschaft and analyzed by Eurofins Umwelt Ost GmbH according to EBC regulations.*

	Biochar	
	as-delivered condition	water-free
Specific surface area (BET) ($m^2\ kg^{-1}$)	-	420.6
TC (%)	56.5	90.3
TOC (%)	56.1	89.7
TN (%)	0.45	0.72
TN ($g\ kg^{-1}$)	4.5	7.2
pH in $CaCl_2$	8.5	-
EC (Electrical Conductivity) (µS cm−1)	601	-
Ca (as CaO) ($g\ kg^{-1}$)	-	18.5
Mg (as MgO) ($g\ kg^{-1}$)	-	1.3
K (as K_2O) ($g\ kg^{-1}$)	-	5.8
P (as P_2O_5) ($g\ kg^{-1}$)	-	0.7
H:$C_{organic}$ molar ratio	0.17	0.17
O:C molar ratio	0.033	0.034

The compost experiment started on July 6th (day 0) and finished on December 1st, 2022 (day 148). Throughout the experiment, the ambient air temperature ranged from 2.4–38.0°C. Therefore, in order to prevent excessive moisture loss (high temperatures in summer) and freezing (cold temperatures in winter) from the compost piles, they were covered with a compost fleece (Toptex 200 g m^{-2}, die natur, Fernitz bei Graz, Austria). Additionally, the boxes were placed on wooden pallets to prevent possible leaching into the soil, as requested by FZJ (Appendix: Figure A.4-5). Both treatments were treated and examined in the same way throughout the whole composting process.

Several adjustments were made during the composting period based on the measured data (Appendix: Figure A.5). On day 34 of composting, WS was added to the outer parts of the piles to improve compost insulation An additional pond liner was placed on top of the boxes on day 75 to prevent uncontrolled water ingress from rainfall into the compost. The piles were turned using garden forks and shovels on days 15, 41, 77 and 108 to homogenize the substrate. This was done to prevent compaction and to protect the edges and corners from drying out, ensuring proper aeration and microbial activity for a homogeneous aerobic composting process.

The turning dates were determined based on the visual impression of the pile, its temperature, moisture and the gas emission data. To maintain an optimum MC between 40–65% and to ensure similar composting conditions between the different replicates, the compost piles were watered on days 34, 37, 41 and 78, following the composting handbook of Rynk et al. (1992).

Various parameters were used to characterize the stability and maturity of the compost and determine the end of the experiment. The GI test was used as an indicator of compost maturity and to assess the absence of phytotoxic compounds. Due to insufficient germination on day 104, the test was repeated on days 126 and 139. Compost temperature, C:N ratio, NH_4^+–N:NO_3^-–N ratio, NH_4^+–N concentrations, pH and electrical conductivity (EC) were also taken into account as indicators of compost quality and stability.

2.2 Sampling of compost and preparation of compost samples

Compost samples were collected on a weekly basis until day 84, and afterwards on days 96, 104, 126, 19, 148. The chemical parameters of the compost were analyzed for samples collected on days 1, 8, 15, 29, 43, 57, 71, 84, 96, 104, 126, 139 and 148. For a representative sampling each sample consisted of six sub-samples taken at different heights at the edge, in the corners and in the centre of the compost pile. Depending on the analysis, fresh, frozen or dried (<50°C) samples were used. Fresh samples were used to monitor the MC and for the germination index (GI) test. Frozen samples were collected and stored within the same day and kept at -20°C until analysis. For the analysis of pH, EC, N_{min}, P_{av} and K_{av}, the frozen samples were ground and homogenized to <5 mm using a hand blender (Philips Pro Mix 3000 series). Dried samples were ground to <2 mm with a shredder and then ball-milled to <1 mm for determination of total nitrogen (TN), total organic carbon (TOC), total organic matter (TOM) and total phosphorus (TP) and potassium (TK) content. To analyze the N retained by bc particles along the compost process, these particles were picked from the compost samples collected on the aforementioned specific days.

The quantification of N_{min}, P_{av}, and K_{av} was conducted at the Central Institute of Engineering, Electronics and Analytics (ZEA-3) at FZJ. All other parameters were measured using equipment provided by IBG-3, following the guidelines established by the Food and Agriculture Organization of the United Nations (FAO) (FAO 2008) and the Association of German Agricultural Analytic and Research Institutes (VDLUFA 2008 and 2014). The methods used for each of these analysis are described in the respective sections below.

2.3 Monitoring of compost parameters

2.3.1 Temperature and moisture

The compost temperature was measured at 18 points of the compost pile, using a G 1700 thermometer equipped with a stainless steel 64 cm-long probe (GTF 40T-620, Greisinger, Remscheid, Germany). Measurements were taken at midday, considering two different heights within the pile, which were adjusted periodically to account for mass loss during composting. Temperature was monitored daily for the first 38 days of composting. Thereafter, temperature was measured three times a week, once a week from day 66 to 99, and on days

110, 127 and 148, which coincided with the days of the gas measurements (Appendix: Table A.2). The FZJ weather station provided the daily ambient air temperature data.

MC was analyzed weekly until day 84 and then on days 96, 104, 126, 139 and 148. MC of the fresh compost samples and bc particles was determined by the gravimetric method based on the weight loss after drying the samples for 24 h at 105°C (FAO, 2008).

2.3.2 Germination Index Test

The GI test was adapted from the method of Zucconi et al. (1981), in which the root elongation and germination percentage of cress seeds in a compost extract is compared with a deionized water control. The aqueous extract of each compost replicate was prepared by shaking 10 g of fresh and homogenized compost with deionized water (1:10 w/v) for 1 h (250 rpm), centrifuging for 15 minutes (3500 rpm) and then filtering with a 0.45 µm syringe filter. For each extract replicate, 10 cress seeds (*Lepidum sativum L.*) were placed in between two filter papers (Whatman 5 filter paper) in a sterilized Petri dish. Thereafter, 5 ml of the germination solution (compost extract or deionized water) was applied to the filter paper and the seeds were incubated for 48 hours at 25°C. The Petri dishes were sealed with parafilm to prevent excessive water loss during the incubation. The germination experiment was carried out on days 104 and 126 with 'Sperli Bio Gartenkresse' and on day 139 with 'Kiepenkerl Kresse', as the Bio seeds could be particularly more sensitive to the extracts. The GI was calculated from the root elongation and the number of germinated seeds as follows:

$$\text{GI (\%)} = \frac{\text{seed germination rate in compost extract} \times \text{root elongation in compost extract}}{\text{seed germination rate in control} \times \text{root elongation in control}} \quad (1)$$

2.3.3 Compost pH and EC

The pH was measured with a glass electrode (WTW Multi 3630 IDS, SenTix940, Xylem Analytics, Weilheim, Germany) using 10 g of homogenized compost samples in a 1:10 (w/v) water extract. The EC was determined with a conductivity meter (WTW Multi 3630 IDS, TetraCon325, Xylem Analytics) using the same water extract (1:10, w/v) after 1 h shaking (250 rpm), 15 min centrifugation (3500 rpm) and filtration (Whatman V2 filter paper). Both methods were carried out according to FAO (2008).

2.4 Nutrient analysis

2.4.1 Nitrogen analysis of compost and biochar particles

For the analysis of N_{min} (NO_3^-–N, NO_2^-–N and NH_4^+–N), the frozen compost samples (4 g) were placed in 50-ml centrifuge tubes and extracted with 0.01 mol L^{-1} $CaCl_2$ (1:10 w/v), 2 h shaking (200 rpm), 15 min centrifugation (3500 rpm) and filtration (0.45 µm syringe filter) according to VDLUFA (2014). The extracts were kept frozen until analysis. NO_3^-–N concentrations were analysed by ion chromatography system (IC850/IC 930 Metrohm, Zofingen, Switzerland). NH_4^+–N and NO_2^-–N concentrations were determined by continuous flow analysis (Alliance Instruments, Salzburg, Austria). All values have been calculated by taking into account a correction factor for the moisture of each frozen sample.

To analyze the N_{min} retained by the bc particles, a three-stage extraction procedure was adapted from Haider et al. (2016), as conventional extractions can underestimate these values. For this, 4 g of the bc were removed as cleanly as possible from the frozen compost samples and placed in 50 ml centrifuge tubes. This extraction method consisted of three steps: Firstly, the bc particles were shaken (200 rpm) in deionized water (1:10, w/v) for 1 h. This was followed by shaking (200 rpm) for 1 h in 2 M KCl (1:10, w/v). Finally, the samples were shaken in 2 M KCl in a water bath for 24 h. During this long-term shaking, the water bath was maintained at 80°C for 8 h. After each shaking step, the entire solution was extracted from the tube with a needle (0.6 mm) to avoid loss of bc. In some of the frozen samples it was not possible to collect a sufficient number of bc particles, but the solid-to-liquid ratio was kept unaltered for extractions. To determine the N_{min} concentrations, the extract was filtered through a 0.45 µm syringe filter and kept frozen until analysis.

An elemental analyzer (Flash EA 2000 coupled with a Delta V Plus, Thermo Fisher Scientific, Bremen, Germany) was used to measure the total nitrogen (TN) concentrations of the dried samples.

2.4.2 Total OM, TOC and available P and K

In order to estimate the content of TOM in the compost, the method of loss of weight on ignition was applied. About 20–30 mg of dried and ball-milled compost was weighed into an ashing vessel and dried at 105°C for 24 h to eliminated water remaining in the samples. The samples were then placed in a muffle furnace and ignited at 550°C for 6 hours. Samples were weighed before and after ignition to determine the percentage of OM. The TOC content was measured using the same elemental analyzer used for TN.

Plant-available potassium (K_{av}) and phosphorus (P_{av}) present in the compost were extracted with 40 ml of a 0.05 mol^{-1} Ca-lactate and Ca-acetate solution (1:20 w/v) after shaking for 90 minutes (200 rpm), centrifuging for 15 minutes (3500 rpm) and filtering (0.45 µm syringe filter) according to VDLUFA (2008). Concentrations were measured by inductively coupled plasma optical emission spectroscopy (iCAP 7600, Thermo Fisher Scientific) and then moisture corrected.

2.5 Data analysis

2.5.1 Estimation of pile dry weight

In order to report the nutrients in the whole compost pile at different days of composting, the compost dry weight for each day of interest was estimated according to Schäfer (unpublished data 2020).
As the weight of the compost piles was only measured on the first day, the theoretical compost weight had to be calculated for the remaining sampling days. The estimated pile dry weight for each sampling day was calculated taking into account the measured OM and the ash content according to the following Equations 2-5:

$$\text{absolute ash amount}_{\text{day 1}}\ (\text{kg dw}) = \frac{(100 - \text{OM}_{\text{day 1}})}{100} \times \text{pile weight}_{\text{day 1}} \qquad (2)$$

$$\text{ash content}_{\text{day x}}\ (\%) = 100 - \text{OM}_{\text{day x}} \qquad (3)$$

$$OM_{day\ x}\ (kg\ dw) = \frac{OM_{day\ x}}{ash\ content_{day\ x}} \times absolute\ ash\ amount_{day\ 1} \quad (4)$$

$$pile\ weight_{day\ x}\ (kg\ dw) = OM_{day\ x} + ash\ amount \quad (5)$$

where day_x is the respective sampling day and $OM_{day\ x}$ (%) is the obtained OM content for this day (2.4.2). As the pile weight of the composting day 1 was known, the absolute ash amount (kg dw) could be calculated. The absolute OM amount (kg dw) was calculated assuming that the absolute ash amount (kg dw) remained constant during the composting period.

The nutrient concentration (mg kg^{-1}) at a specific sampling date was multiplied by the corresponding calculated theoretical compost weight for the same sampling date in order to obtain the nutrient amount per compost pile.

2.5.2 Determination of losses of OM, TOC, TN, available P and K

The losses of TOM, TOC, TN, TP and TK from day 1 to day 148 of composting were calculated according to equation 5.

$$Loss\ (\%) = \left(\frac{W_1C_1 - W_{148}C_{148}}{W_1C_1}\right) \times 100 \quad (6)$$

Where, compost dry weight (kg) at day 1 (W_1) and at the last day (W_{148}) of the experiment and the concentration of the nutrient (mg kg^{-1} dw) at these respective days: day 1 (C_1) and day 148 (C_{148}).

2.6 Gas Fluxes during composting

2.6.1 CO_2, N_2O and CH_4 flux measurements

Gas samples were taken three times per week until day 67, twice a week until day 81 and then on days 85, 92, 99, 110, 127 and 148 of composting (Appendix: Table A.2). Fluxes of CO_2, N_2O and CH_4 were measured using the static chamber-based method. For that, four cylindrical PVC tubes (25 cm height, 11 cm diameter) were used as chambers in each of the compost piles to enhance the representativity of gas sampling (Appendix: Figure A.6). Together, the four chambers (0.038 m^2) covered 5.3% of compost surface area (0.72 m^2). During sampling, the tubes were sealed with a screwable PVC lid equipped with a rubber to trap the gases emitted by the compost inside the chamber. Each lid was equipped with one septum for gas sampling with a syringe, and two cable entries (2–7mm); one for insertion of thermometer (for temperature measurement into the chamber) and one for a flexible 1/8" vent tube used for pressure equilibration inside the chamber during gas sampling. In each compost box, gas samples were taken from the headspace of each of the four chambers at four time points within the same sampling day using a 50 ml polypropylene syringe. The gas mixture (10, 20 or 30 ml) of the four chambers at individual time points was immediately transferred to a 22-ml pre-evacuated gas chromatography glass vial closed with an aluminium cap and a butyl rubber septum. The gas concentration at each time point was analyzed on a gas chromatograph (Chromatograph Electron Capture Detector/Flame Ionization Detector (Clarus 580, PerkinElmer, Rodgau, Germany). On each sampling day, the headspace of the tube was adjusted by correcting the insertion depth of the tube in the compost to ensure equal sampling conditions across the compost boxes over composting time with its accompanying compost mass loss The increase in

gas concentration over time (obtained from the four sampling time points) was used to calculate flux rates, taking into account the headspace and the amount of gas collected (Equation 6). In the course of the composting process and based on the gas fluxes data obtained, the intervals of the four sampling time points and days of sampling were adjusted (Appendix: Table A.2). In general, the four sampling intervals consisted of 5, 10, 15 and 20 minutes at the beginning of the experiment, and were extended to 45, 90, 135 and 180 minutes at later stages of the composting process.

The GHG fluxes (μg m^{-2} h^{-1}) were calculated according to the following equation:

$$GHG_{flux} = \frac{S}{1{,}000{,}000} \times \frac{PV}{RT} \times \frac{M}{A} \quad (7)$$

where S is the slope of the increase in gas concentration with time (ppm h^{-1}), to convert ppm (μ L^{-1}) to L^{-1} it is divided by 1,000,000 (or 1,000 to convert to ppb), P is the atmospheric pressure in the chamber (1 atm), V is the chamber headspace (L), R is the universal gas constant (0.0831446 atm L moL^{-1} K^{-1}), T is the temperature measured in the chamber at final syringe sampling step (K), M the molar mass of C or N (g moL^{-1}) and A is the basal area of the chamber (m^2). The slope (S) was set to zero if R^2 <0.81 as it was considered to be not significant.

2.6.2 Cumulative CO_2, N_2O and CH_4 fluxes

Cumulative emissions were calculated by multiplying the average GHG flux rate of two consecutive measurement days by the number of days separating them, and adding this to the previous cumulative data. The resulting gas flux data of the entire composting period were summed up and presented as total g CO_2-C m^{-2}, mg CH_4-C m^{-2} and mg N_2O-N m^{-2} emissions.

2.6.3 Global warming potential

The global warming potential (GWP) was calculated according to equation 8:

$$Q_{GWP} = \left(Q_{CH_4} \times 28 \times \frac{16}{44}\right) + \left(Q_{N_2O} \times 265 \times \frac{12}{28}\right) + Q_{CO_2} \quad (8)$$

where Q_{GWP} is the total amount of GWP expressed in units CO_2-C equivalents, Q_{CO_2} is the cumulative amount of g CO_2-C m^{-2} emitted during the composting, Q_{N_2O} the total amount of g N_2O-N m^{-2} and Q_{CH_4} the total amount of g CH_4-C m^{-2}. The conversion factors (28 and 265) are based on the latest reported values of AR5 (Fifth Assessment Report of the IPCC) on a 100-year time horizon without climate-carbon feedback and adapted to the conversion of N2O-N and CH4-C in CO2-C (IPCC, 2013).

2.7 Composting-induced aging of biochar assessed by ^{13}C-NMR

In order to verify shifts in the chemical structure of bc particles induced by co-composting with the organic residues, bc particles picked from compost at day 77 (Bc77) and 148 (Bc148) of composting, as well as the original biochar (OriBc) were analyzed by solid-state ^{13}C-nucler magnetic resonance spectroscopy (^{13}C-NMR). The Bc77 and Bc148 samples consisted of composite samples of bc particles collected from the three bc compost boxes replicates.

For the ^{13}C-NMR analysis, OriBc, Bc77 and Bc148 samples were crushed into fine particles in a mortar and packed into zirconium rotors. The ^{13}C-NMR spectra of bc samples were obtained with a Bruker Avance Neo 600 Mhz spectrometer (Bruker BioSpin GmbH) working at a ^{13}C frequency of 150.81 MHz. Cross polarization magic angle spinning was applied with a spinning speed of 18 kHz and achieved during a contact time of 500 µs with a ramped ^{1}H pulse. The relaxation delay was 2 s, the pulse width was 4.5 µs and 2048 scans were accumulated.

The ^{13}C chemical shifts were calibrated relative to tetramethylsilane (0 ppm) and glycine (COOH at 176.08 ppm). The assignments of the chemical regions of the ^{13}C-NMR spectra were performed according to De la Rosa et al. (2018) and Knicker et al. (2005) as follows: -10–45 ppm (alkyl C); 45–60 ppm (N-alkyl C); 60–90 ppm (O-alkyl C); 90–140 ppm (aryl C); 140–160 ppm (O/N-aryl C); 160–190 ppm (carboxyl C). The integration of the total ^{13}C signal intensity (100%) was performed using MestreNova software by summing up the areas in the spectrum of all aforementioned chemical groups. Then, the proportional contribution (%) of each chemical C group to the total ^{13}C intensity was calculated taking into account the spinning sideband disturbance (Knicker et al., 2005). The aromaticity index of the bc was obtained as the aryl C (90–140 ppm)/alkyl C (-10–45 ppm) ratio according to De la Rosa et al. (2018). The hydrophobicity index (Abelmann et al., 2005) of bc was calculated as (aryl C + alkyl C)/(carboxyl C + O-alkyl C).

2.8 Statistical Analysis

The data is presented as mean ± standard error (SE) (n=3). The means of ctrl and bc were compared statistically by t-test ($P < 0.05$). The analysis and visualization of the collected data was conducted with the RStudio software (Version 4.2.3 RStudio, PBC).

3. Results

3.1 Compost observation

A visual impression of compost piles at day 0, 41 and 148 is provided in Figure 1. From beginning to end of composting, compost volume decreased by 74.3% (ctrl) and 68.6% (bc) (Appendix: Figure A.7). On days 63 and 70, precipitation entered the boxes through the compost fleece, creating visible but sporadic leaching (not analyzed). As not all boxes were equally wet, the moisture across the boxes was adjusted by manually adding water to the drier boxes. On day 75, pond liner was installed over the compost fleece and prevented further precipitation entering the compost boxes, thus no further evidence of nutrient loss due to large amounts of leachate were detected. No animal intrusion into the compost piles was observed, probably because of the mesh wires surrounding the sides and bottom of the boxes and the coverage of the boxes with compost fleece and pond liner. Partially compact, undecomposed straw was visible in the boxes when the compost was turned on day 77.

Figure 1 *Compost observation at day 0 (left picture) with temperature measurement, day 41 (middle) before second turning and 148 (right picture) on the last day.*

3.2 Control parameters

3.2.1 Compost temperature and composting phases

Average compost temperature as well as ambient temperature are shown in Figure 2. Both treatments (bc and ctrl) underwent the four phases of composting: mesophilic I (<45°C), thermophilic phase (≥45°C), mesophilic phase II (<45°C) and maturation phase (close to ambient temperature). On day 0, when the compost boxes were filled with the mixture of feedstocks, the mean temperature of compost ranged between 37.9°C and 41.2°C (Figure 2).

A rapid increase in compost temperature was detected in both treatments after day 0 of composting, marking the transition from the mesophilic phase I to the thermophilic phase (Figure 2). The thermophilic phase started on the first day after the mixing and lasted for a period of 18 days. Within the thermophilic phase, maximum compost temperatures were 71.0°C in ctrl and 71.5°C in bc treatment at day 4 of composting (Figure 2). Right after the first compost turning (day 15), of composting, compost temperature increased slightly in both treatments, which also coincided with the raising of the ambient air temperature (Figure 2). The compost hygienization phase (>55°C) within the thermophilic phase lasted 8 days (from day 1 to day 8 of composting) in both treatments (Figure 2). During the subsequent composting phase, the mesophilic phase II, the compost temperature decreased almost continuously and lasted for

66 days in both treatments (Figure 2). From day 85 of composting until the end of the composting period the compost temperatures were stable (between 7.6 and 15.6°C) and close (±3°C) to ambient air temperatures (Figure 2). Furthermore, even after two compost turning events on days 77 and 108, no elevation of compost temperature was noticed, regardless of treatment. Together, these data indicated the start of the maturation phase of compost, which lasted for 64 days until the end of the composting experiment. Final compost temperatures ranged between 7.4°C and 7.9°C.

Turning the piles on days 15, 41, 77 and 108 did not significantly increase the temperature in the piles. However, by turning and homogenizing the compost piles, temperature differences within the pile were equalized between the warmer centre (up to 36.1°C on day 9) and colder edges. Comparing the temperature patterns of the two treatments in all compost phases, no significant difference can be observed due to the presence of the bc.

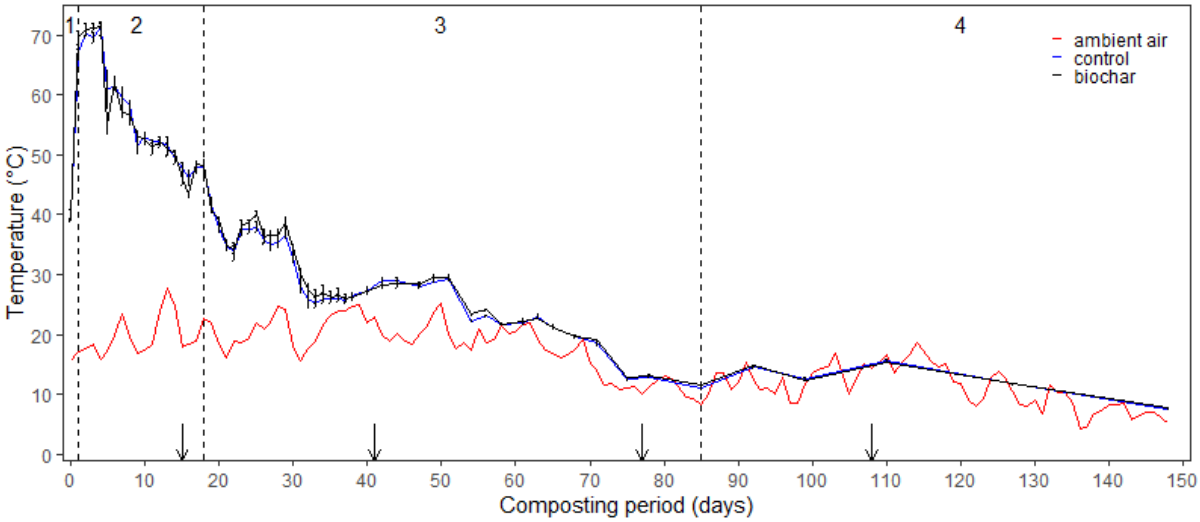

Figure 2 *Ambient air temperature and compost temperature in control and biochar treatments over the composting period. Values are reported as mean (n=3) and error bars show standard error. Dashed vertical lines indicate the following composting phases: (1) mesophilic phase I (<45°C), (2) thermophilic phase (≥45°C), (3) mesophilic phase II (<45°C) and (4) maturation phase (close to ambient temperature). Arrows indicate compost pile turning events.*

3.2.2 Moisture content

The initial MC of the compost was 74.9% in the ctrl and 74.2% in the bc treatment, decreasing to final values of 54.2% in the ctrl and 55.5% in the bc on day 148 (Figure 3a). The greatest drop in compost MC occurred right at the beginning of composting (from day 1 to day 8) in both treatments (Figure 3a). The initial MC was above the recommended range of 40–65% mostly because of the high MC of the kitchen waste (91.8%). In the further course of composting, the mean MC of compost in both treatments remained within the recommended range (Figure 3a). The loss of water by evaporation or sporadic leaching (not quantified) and MC heterogeneity within compost treatment were compensated by manual watering of the piles with distilled water. Biochar had no significant effect on compost MC, regardless of days of composting.

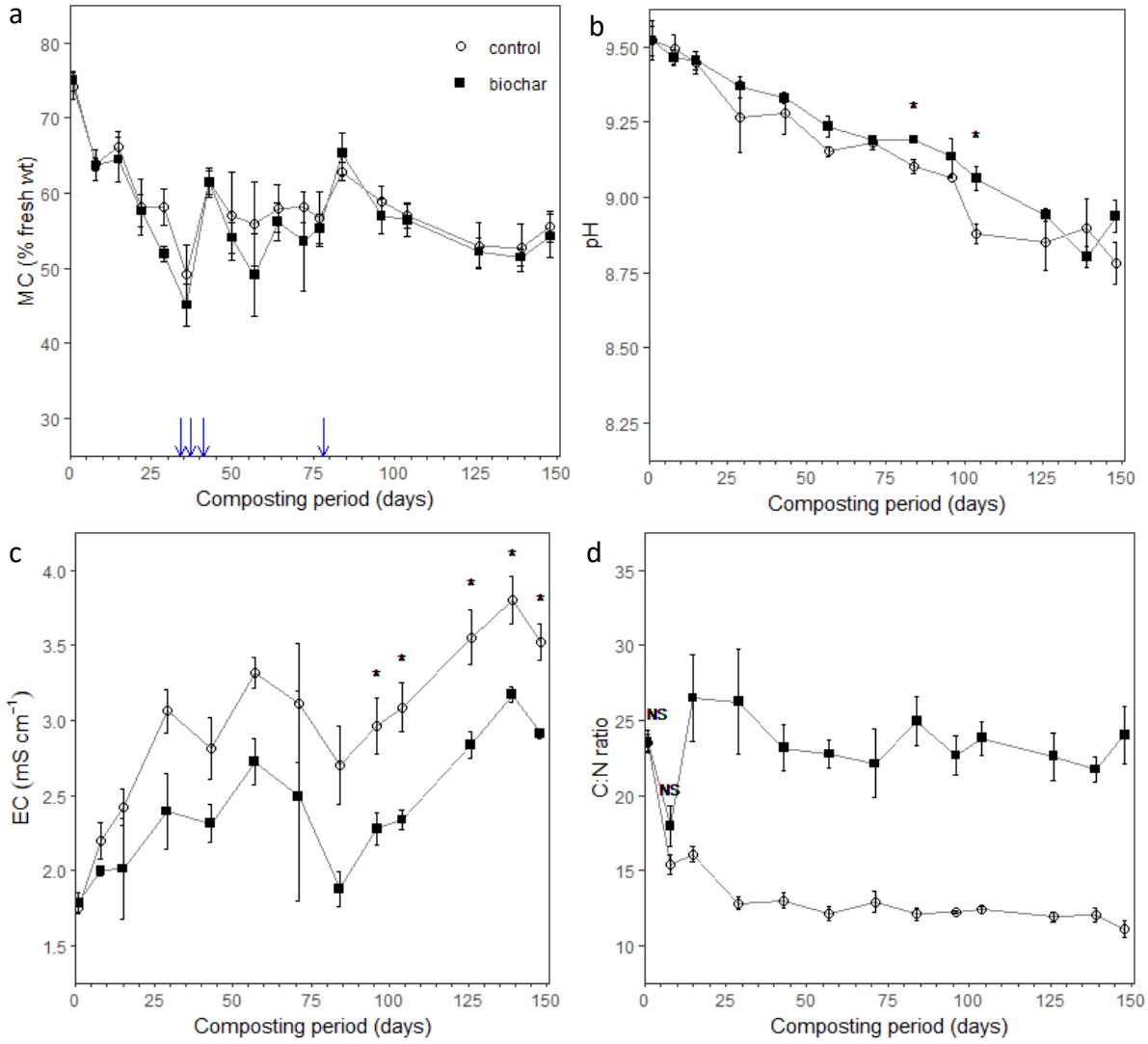

Figure 3 *Control parameters during the composting process. a) Moisture content (MC), b) pH c) electrical conductivity (EC), d) C:N ratio. Blue arrows indicate watering events of compost piles. In figure "a" statistical differences were not detected. In figures "b" and "c" asterisks (*) indicate significant (p<0.05) difference between treatments. In figure "d" NS indicate no significant difference, otherwise control and biochar treatments differed statistically (p<0.05).*

3.2.3 Compost pH and EC

The pH decreased gradually during composting in both treatments from initial values of 9.5 to final values of 8.8 (ctrl) and 8.9 (bc) (Figure 3b). In the mesophilic phase II and in the maturation phase there is a tendency for higher pH values in the BC amended compost, but only on composting days 84 and 104 they are significantly higher (Figure 3b). The final pH in bc (8.9) and ctrl (8.8) did not differ statistically.

The initial (day 1) EC was 1.8 mS cm^{-1} and tended to increase with the composting time in both ctrl and bc (Figure 3c). Between days 57 and 84, the EC decreased from 3.3 to 2.7 mS cm^{-1} in ctrl and from 2.7 to 1.9 mS cm^{-1} in bc, and these values increased to 3.5 mS cm^{-1} (ctrl) and 2.9 mS cm^{-1} (bc) in the final compost. From day 96 up to the last day of composting, EC was significantly higher in the ctrl than in bc (Figure 3c).

3.2.4 C:N ratio

The C:N ratio of compost at day 1 of composting was 24 in both ctrl and bc treatments (Figure 3d). During the first week of composting, the C:N ratio in ctrl and bc dropped to 15.4 and 18, respectively, but did not differ statistically (Figure 3d). In the ctrl, the C:N ratio decreased steadily until the final measurement (11.1) (Figure 3d). This decrease was more pronounced during the thermophilic phase and less in the mesophilic phase II and the maturation phase. In contrast, the C:N ratio in bc treatment increased to 26.5 on day 15 and remained relatively stable until the final measurement (24.0) (Figure 3d). For this time frame, the C:N ratio of compost was statistically higher in bc than in ctrl (Figure 3d).

3.3 TOM and nutrient dynamics

3.3.1 TOM

In general, both treatments exhibited a continuous decrease in TOM during the composting process (Figure 4a). The decrease of the initial TOM until the end of the composting period was more evident in the ctrl (82.3 to 72.4%) than in the bc treatment (82.5 to 79.3%) (Figure 4a). In the ctrl treatment, the TOM decreased remarkably until the beginning of the mesophilic phase II and remained mostly unchanged until compost finalization (Figure 4a). In the bc treatment, the greatest decrease in TOM was observed at the beginning of the thermophilic phase (Figure 4a), and afterwards TOM remained practically unaltered until the end (Figure 4a). Except for days 1, 8 and 71 of composting where TOM of ctrl and bc did not differ, TOM was always statistically higher in bc treatment (Figure 4a). From the beginning until the last composting day, the OM losses ranged from 35.2-53.4% (ctrl) and 11.8–23.3% (bc), with significantly higher losses in the ctrl compost than in bc (Table 4). Compost pile dry weight decreased from 71.3 to 46.1 kg in ctrl and from 82.0 to 69.3 kg in the bc (Figure 4b), and was about 44.7% higher in bc across the whole composting period.

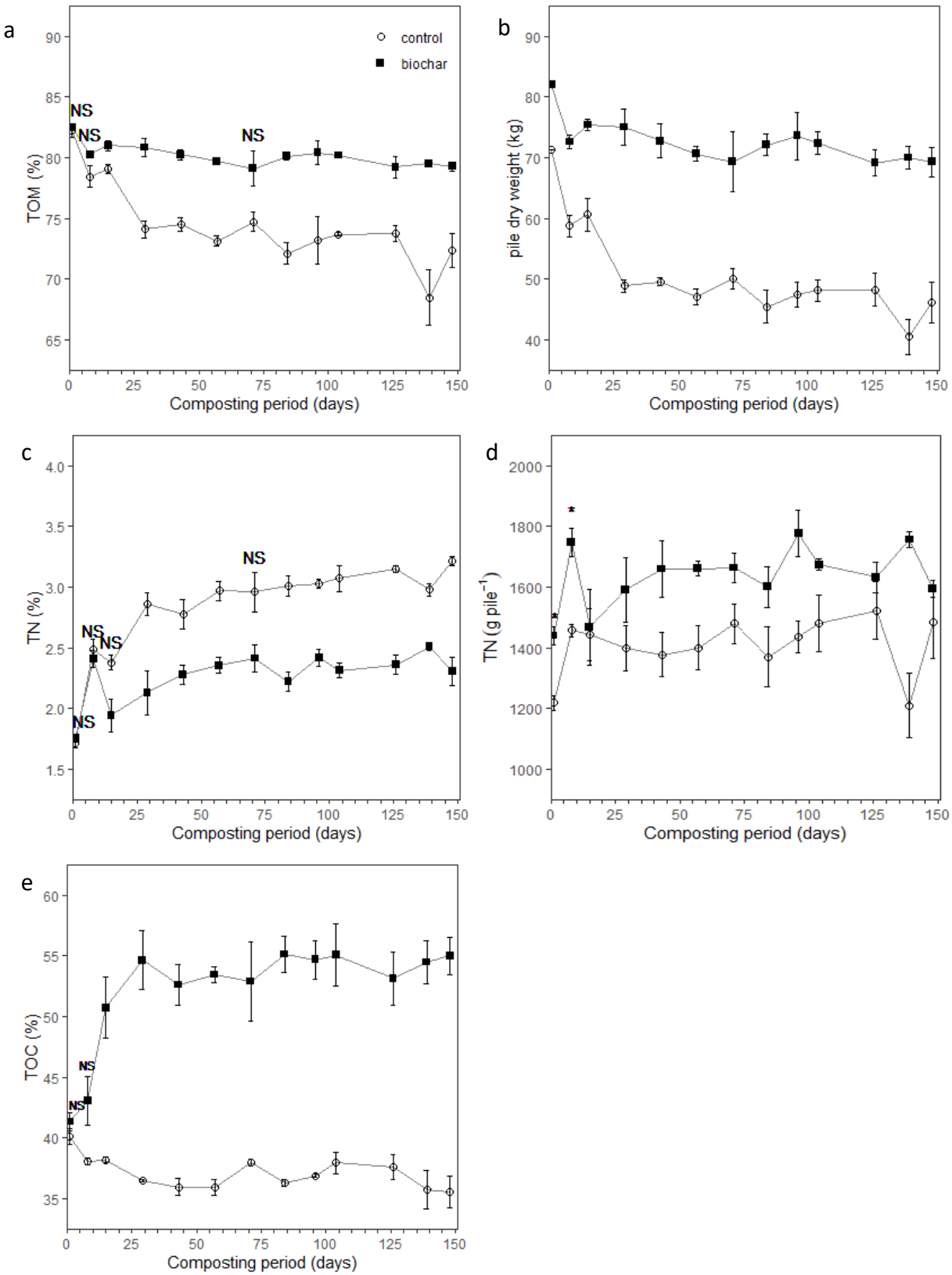

Figure 4 *Control parameters during the composting process. a) Total organic matter (TOM), b) Pile dry weight, c) Total nitrogen (TN), d) Total nitrogen in compost pile (g pile^{-1}), e) Total organic carbon (TOC). Values are mean ± SE (n=3).In figures "a", "c" and "e" NS indicate no significant difference, otherwise control and biochar treatments differed statistically ($p<0.05$). In figure "b" statistical differences was detected in all dates. In figure "d" asterisks (*) indicate significant ($p<0.05$) difference between treatments.*

Table 4 *Physical and chemical parameters of the initial (day 1) and final compost (day 148).*

	Day 1		Day 148	
	control	biochar	control	biochar
MC (% fresh wt)	74.2 ± 1.6	74.9 ± 1.2	55.5 ± 1.9	54.2 ±2.6
pH	9.5 ± 0.1	9.5 ± 0.1	8.8 ± 0.1	8.9
EC (mS cm^{-1})	1.8	1.8 ± 0.1	3.5 ± 0.1	2.9
TOM (%)	82.3 ± 0.5	82.5 ± 0.2	72.4 ± 1.1	79.3 ± 0.3
TOC (%)	40.2 ± 0.5	41.3 ± 0.6	35.6 ± 1.1	55.0 ± 1.2
TN (%)	1.7 ± 0	1.8 ± 0	3.2 ± 0	2.3 ± 0.1
TN_{av} (mg kg^{-1})	114.9 ± 5.7	118.2 ± 5.7	287.7 ± 15.9	290.5 ± 7.9
C:N	23.5 ± 0.5	23.6 ± 0.6	11.0 ± 0.4	24.0 ± 1.6
NH_4^+–N (mg kg^{-1})	114.9 ± 5.7	118.2 ± 5.7	31.5 ± 3.3	29.0 ± 6.7
NO_3^-–N (mg kg^{-1})	0	0	256.1 ± 12.8	261.5 ± 11.6
P_{av} (mg kg^{-1})	246.2 ± 14.8	252.7 ± 21.3	1396.1 ± 190.6	1003.1 ± 86.6
K_{av} (mg kg^{-1})	1601.5 ± 36.2	1706.4 ± 121.0	9906.6 ± 1222.6	6759.1 ± 214.0
TN loss (%)	-	-	-21.4 ± 6.4	-10.7 ± 0.8
TOM loss (%)	-	-	42.8 ± 4.4	18.7 ± 2.9
TOC loss (%)	-	-	42.8 ± 3.1	-12.7± 5.3

3.3.2 TOC

At day 1 of composting the TOC in ctrl and bc were 40.2 and 41.3%, respectively, and did not differ statistically (Figure 4e). In the ctrl compost, TOC decreased significantly to 35.6%, with losses between 37.8 to 50.2% while considering the mass loss of the compost (Table 4). Whereas, in the bc treatment the TOC increased during composting, mainly until the beginning of mesophilic phase II, and reached 55% as final TOC (Figure 4e). The TOC content in bc were significantly higher compared to the ctrl from day 15 of composting onwards (Figure 4e).

3.3.3 TN

At day 1 of composting, TN concentrations in ctrl and bc were 1.7 and 1.8%, respectively (Figure 4c). The TN concentration in ctrl and bc did not differ statistically until day 29 (Figure 4c). Throughout the composting process, the TN concentrations in ctrl and bc increased up to final concentrations of 3.2 and 2.3% in ctrl and bc, respectively, and were significantly higher in ctrl (except for day 71) (Figure 4c). When analysing the TN concentration normalized by pile weight, the TN (g $pile^{-1}$) tended to be greater in bc than in ctrl (Figure 4d). However, these differences were significant only until day 8 of composting (Figure 4d). Taking into account the pile mass loss, negative values of TN were calculated which suggest a net N gain of 21.4 and 10.7% in the ctrl and bc treatment, respectively, throughout the composting (Table 4).

3.3.4 Plant-available phosphorus and potassium

On day 1 of composting, the amount of P_{av} was 246.2 mg kg^{-1} (17.4 g $pile^{-1}$) in the ctrl and 252.7 mg kg^{-1} (20.7 g $pile^{-1}$) in the bc treatment (Figure 5a and b). Throughout the composting process, the amount of P_{av} increased in both treatments, and was at the end of composting significantly higher in ctrl (1396.1 mg kg^{-1}) than in bc (1003.3 mg kg^{-1}) (Figure 5a). Considering the loss of pile dry weight during composting, there was a tendency for a higher concentration of P_{av} (g $pile^{-1}$) in the bc treatment, but this was only significant at day 57 (Figure 5b). The final P_{av} values in ctrl and bc were 64.8 and 70.0 g $pile^{-1}$ and did not differ statistically (Figure 5b).

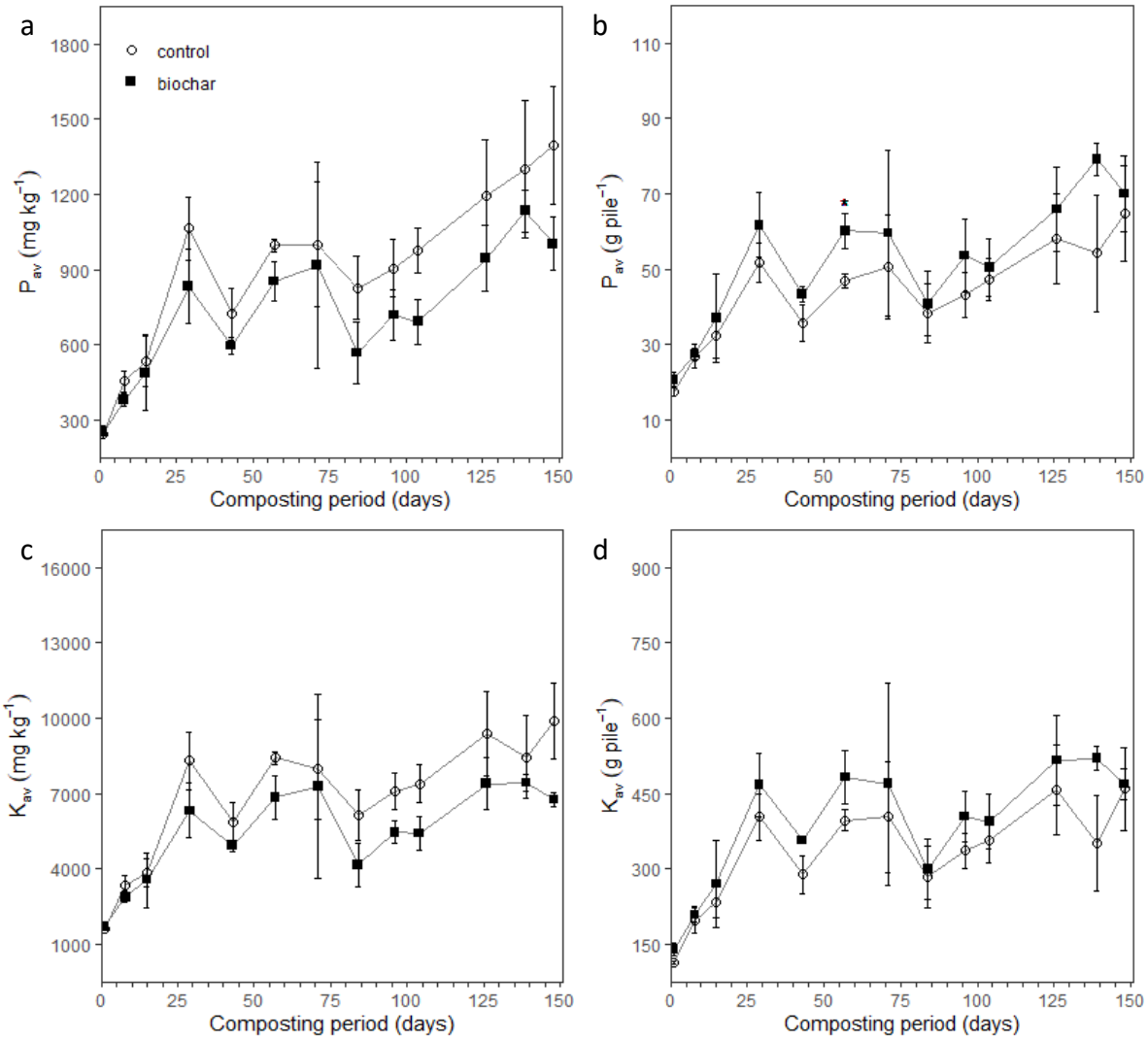

Figure 5 *Plant-available phosphorus (P_{av}) and potassium (K_{av}) dynamics during the composting process. a) plant-available P concentration (P_{av}) (mg kg^{-1}), b) plant-available P (P_{av}) in the compost pile (g $pile^{-1}$), c) plant-available K concentration (K_{av}), d) plant-available K (K_{av}) (g $pile^{-1}$). Values are mean ± SE (n=3). In figures "a", "c" and "d" no statistical differences was detected. In figure "b" asterisks (*) indicate significant ($p<0.05$) difference between treatments.*

Similar dynamics could be seen in the amounts of total K_{av} with initial values of 1601.5 mg kg^{-1} (114.1 g $pile^{-1}$) in ctrl and 1706.4 mg kg^{-1} (139.9 g $pile^{-1}$) in bc treatment. The values in the final compost were 9906.6 mg kg^{-1} (459.2 g $pile^{-1}$) and 6759.1 mg kg^{-1} (469.1 g $pile^{-1}$), in ctrl

and bc, respectively (Figure 5c and d). No statistical differences for K_{av} occurred between the two treatments throughout composting (Figure 5c).

3.4 Mineral nitrogen dynamics

The dynamics of N_{min} forms (NH_4^+–N, NO_2^-–N and NO_3^-–N) in ctrl and bc along composting are illustrated in Figure 6a-f. Initially, on day 1, NH_4^+–N concentrations peaked at 114.9 mg kg^{-1} in ctrl and 118.2 mg kg^{-1} in bc, and subsequently decreased continuously until the end of the composting period in both treatments (Figure 6a).

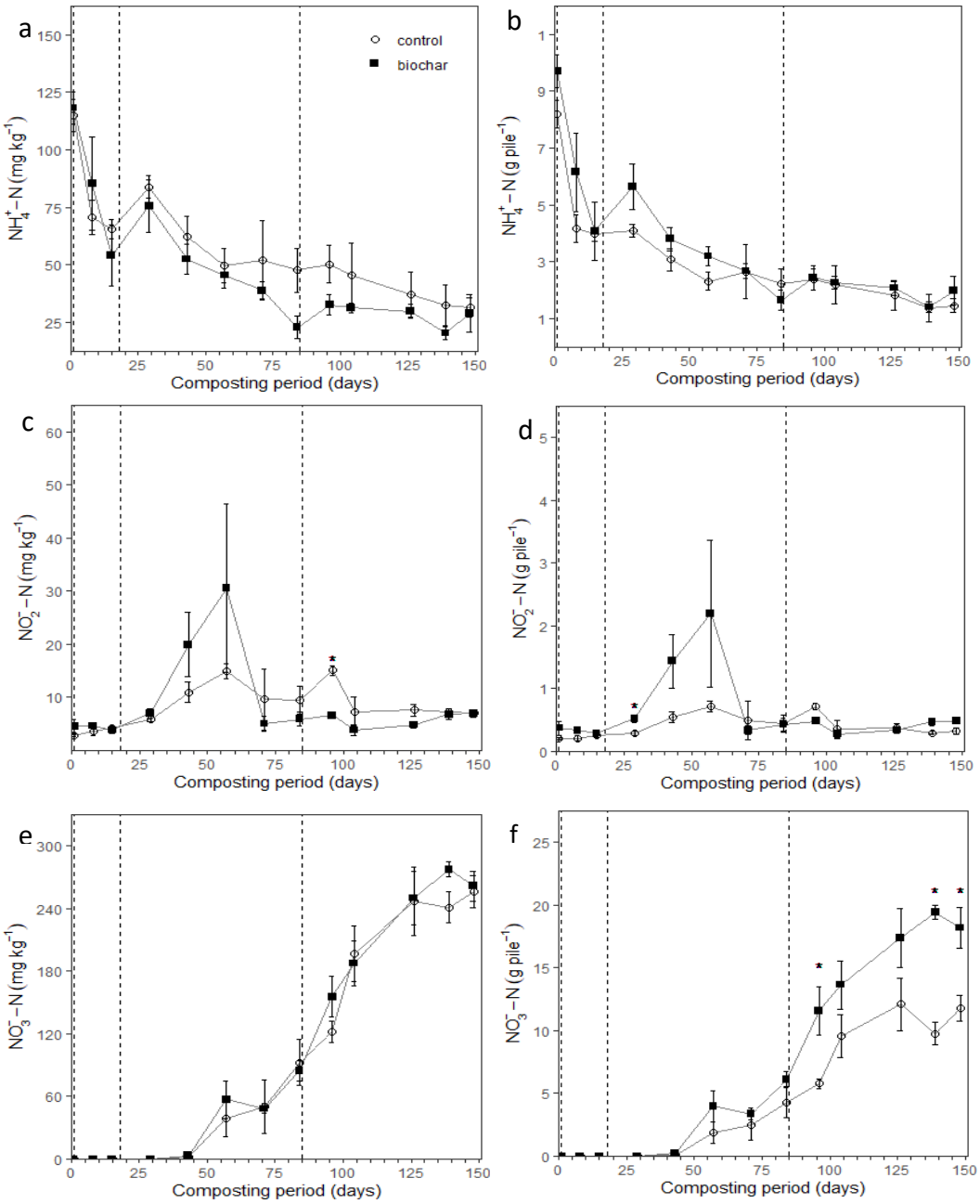

Figure 6 *Mineral nitrogen dynamics during the composting process. a) NH_4^+–N (mg kg^{-1}), b) NH_4^+–N in compost pile (g $pile^{-1}$), c) NO_2^-–N (mg kg^{-1}), d) NO_2^-–N in compost pile (g $pile^{-1}$), e) NO_3^-–N (mg kg^{-1}), f) NO_3^-–N in compost pile (g $pile^{-1}$). Values are mean ± SE (n=3). In figures "a", "b", "d" and "e" no statistical differences was detected. In figures "c" and "f" asterisks (*) indicate significant (p<0.05) difference between treatments.*

More specifically, in the thermophilic phase, there was a rapid decline in extractable NH_4^+–N. After a transient increase on day 29, NH_4^+–N (mg kg^{-1}) concentrations showed a relatively continuous decline during the mesophilic phase II and the maturation phase in both treatments (Figure 6a). Throughout the composting process, the NH_4^+–N (mg kg^{-1}) and g $pile^{-1}$), did not differ statistically between ctrl and bc (Figure 6a and b). In the final compost, NH_4^+–N concentrations in ctrl and bc were 31.5 and 29 mg kg^{-1}, respectively (Figure 6a). Although a slight trend towards higher NH_4^+–N concentrations was observed in the ctrl treatment, normalized values tended to be higher in the bc treatment due to reduced mass loss (Figure 6b).

In both treatments, NO_3^-–N was undetectable until day 37 (Figure 6e). In the mesophilic phase II nitrification initiated. Initially, this was reflected in an increase in NO_2^-–N concentrations on day 29 (Figure 6c), followed by a subsequent increase in NO_3^-–N concentrations after day 36 (Figure 6e), in both treatments (Figure 6e and f). After the second turning (day 41) of compost piles, an increase in extractable NO_2^-–N (mg kg^{-1}) was observed with a more pronounced peak in the bc treatment (30.6 mg kg^{-1}) on composting day 57 (Figure 6c). A significantly higher peak in NO_2^-–N concentrations in ctrl treatment (15.0 mg kg^{-1}) was measured after the third turning on day 96 compared to bc (Figure 6c). Except from day 96, NO_2^-–N concentrations were not significantly different between the ctrl and bc treatment.

As the composting process progressed and the compost matured, the concentrations of NO_3^-–N continued to rise steadily until the end of the composting period in both treatments (Figure 6e and f). The final ctrl and bc compost have NO_3^-–N concentrations of 256.1 mg kg^{-1} and 261.5 mg kg^{-1} without a significant difference (Figure 6e). It is important to highlight that NO_3^-–N (g $pile^{-1}$) in bc was significantly higher than in ctrl at days 96 and 136, as well as in the final compost (54.2% higher in bc) (Figure 6f).

Available N_{min} (sum of NH_4^+–N and NO_3^-–N) increased during composting from initial concentrations of 114.9 mg kg (ctrl) and 118.2 mg kg^{-1} (bc) to final values of 287.5 mg kg^{-1} (ctrl) and 290.5 mg kg^{-1} (bc). No significant difference in available N between the two treatments was observed, suggesting that both treatments produced similar results in terms of N availability.

3.5 Nitrogen retention by biochar particles during composting

The highest amount of NH_4^+–N (116.8 mg kg^{-1}) retained in bc particles during composting was extracted at day 1 with water (Figure 7a). The water-extracted NH_4^+–N remained between 19.2 and 27.5 mg kg^{-1} between days 8 and 43 and tended to decrease to 8.4 mg kg^{-1} thereafter until compost finalization (Figure 7a). The second extraction step (with 2 M KCl) only extracted NH_4^+–N at day 1 (50.3 mg kg^{-1}), subsequently values were below detection limit (Figure 7a). The initial values of strongly bound NH_4^+–N were 43.4 mg kg^{-1} and thereafter remained between 17.6 and 25.3 mg kg^{-1}, with a final concentration of 24.4 mg kg^{-1} (Figure 7a). The percentage distribution of NH_4^+–N intro extraction steps over days of composting show a clear transition from predominantly plant-available (55.2%) NH_4^+–N at the beginning of composting to predominantly tightly bound (74.7%) NH_4^+–N at the final composting stage (Figure 7b).

NO_2^-–N concentrations tended to increase from day 1 to day 43, regardless of the extraction step, with peak concentrations of 7.0 mg kg^{-1} (water-extract), 2.5 mg kg^{-1} (KCl extract) and 6.3 mg kg^{-1} (strongly bound) (Figure 7c). Thereafter, the NO_2^-–N recovered in all extraction steps tended to decrease (Figure 7c). During the initial stages of the composting process, NO_2^-–N

could be predominantly extracted with water (70.7%) (Figure 7d). However, after day 29, a greater proportion of NO_2^-–N appeared to be more tightly bound to bc (Figure 7d). At the final day of composting, about 23, 17 and 60% of the total extractable NO_2^-–N was extracted with water, 2 M KCl and 2 M KCl (long-term shaking), respectively (Figure 7d).

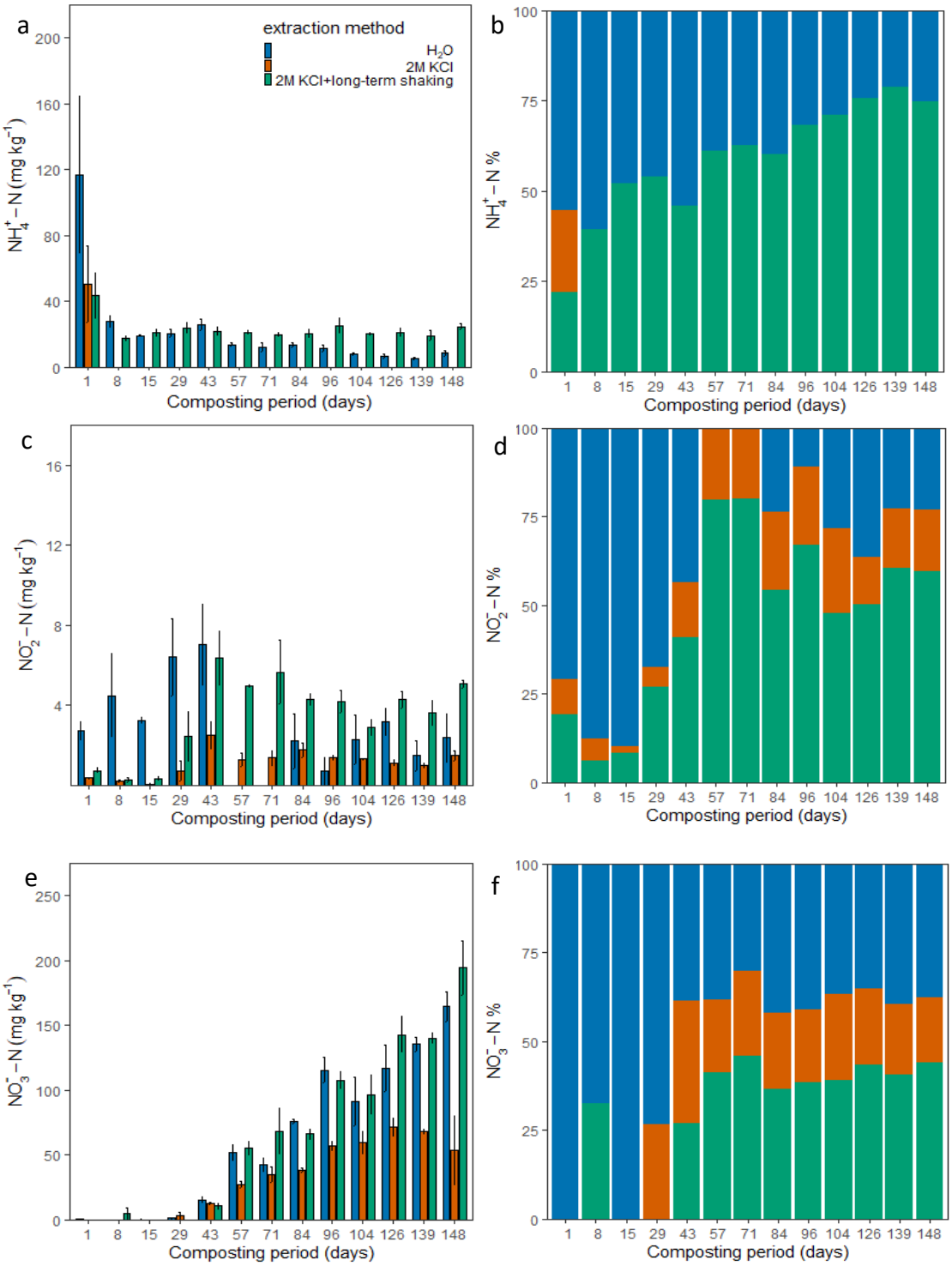

Figure 7 *Mineral nitrogen retention by biochar particles with three extraction methods. a) NH_4^+–N concentration, b) NH_4^+–N percentage distribution, c) NO_2^-–N concentration, d) NO_2^-–N percentage distribution, e) NO_3^-–N concentration, f) NO_3^-–N percentage distribution. All values are reported as mean ± SE (n=3).*

Until day 29 of the experiment, only negligible amounts of NO_3^-–N were extracted from the bc particles (Figure 7e). From day 43 to compost finalization, an upward trend in NO_3^-–N concentrations was observed across all extraction steps (Figure 7e). In the final compost, NO_3^-–N extracted with water (164.4 mg kg^{-1}), 2M KCl (80.0 mg kg^{-1}) and 2M KCl long-term shaking (194.3 mg kg^{-1}), corresponded to 37, 19 and 44% of total NO_3^-–N retained by the bc particles (Figure 7f). This distribution remained practically unaltered since day 84 of composting.

In the final compost, the total summed content of NH_4^+–N and NO_3^-–N retained by the bc particles was 471.4 mg kg^{-1}, of which 37% is readily available and 46% is strongly bound to bc.

3.6 ^{13}C-NMR characterization of original and aged biochar

In general, the ^{13}C NMR spectra of original and aged bcs were similar and strongly dominated by aryl C (aromatic C forms) (Figure 8).

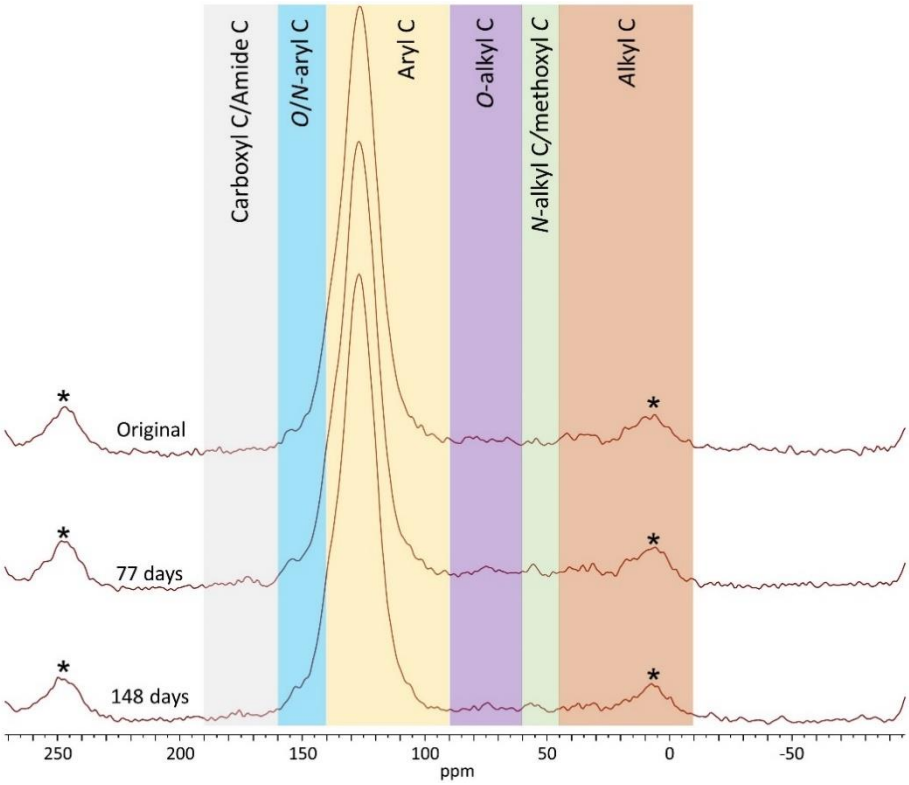

Figure 8 *Solid state ^{13}C-NMR spectra of original biochar and the same biochar aged by co-composting with organic waste for 77 and 148 days. Asterisks refer to spinning side bands, which were considered while calculating the relative intensity of the chemical groups.*

The contribution of aryl C to the total ^{13}C intensity gradually decreased with aging as follows: OriBc (84.3%) > Bc77 (81.8%) > Bc148 (79.3%) (Table 5). Oppositely, the alkyl C contribution to the ^{13}C total intensity gradually increased with aging, OriBc (2.4%) < Bc77 (2.9%) < Bc148 (4.0%), although these shifts were less evident compared to that in aryl C (Table 5). As result of the shifts in aryl C and alkyl C contribution to total ^{13}C intensity caused by aging of bc, the aromaticity index (aryl C/alkyl C) of bc decreased considerably with aging, especially after the second half of composting period, as follows: OriBc (35) > Bc77 (30) > Bc (20). Although the contribution of carboxyl C, O/N-aryl C, O-alkyl C and N-alkyl C tended to increase as signal of

bc aging, these changes were minimal (<1.2%) even after 148 days of bc co-composting (Table 5).

Table 5 *Relative intensity distribution (%) in the solid-state ^{13}C NMR spectra of original biochar (OriBc) and the same biochar aged for 77 (Bc77) and 148 (Bc148) days via co-composting.*

	Spectrum region (ppm)					
	190–160	160–140	140–90	90–60	60–45	45–(-10)
	Carboxyl C	O/N-aryl C	Aryl C	O-alkyl C	N-alkyl C/methoxyl C	Alkyl C
OriBc	1.4	8.5	84.1	2.5	1.1	2.4
Bc77	1.6	8.6	81.8	3.2	1.8	2.9
Bc148	2.2	9.6	79.3	3.1	1.9	4.0

3.7 Dynamics of greenhouse gas emissions

3.7.1 Temporal CO_2, CH_4 and N_2O emissions

The temporal dynamics of GHG emissions is shown in Figure 9a. There is a pattern of high emissions at the beginning, which is followed by a decrease as composting progresses. The highest peaks of CO_2 flux along the whole experiment occurred within the thermophilic phase, at day 1, where CO_2 fluxes were 11904.6 mg CO_2-C m^{-2} h^{-1} in ctrl and 13372.9 mg CO_2-C m^{-2} h^{-1} in bc (Figure 9a), corresponding to 255.6 to 336.9 g CO_2-C m^{-2} day^{-1}, respectively, without statistical differences. After the initial emission peak, a gradual decrease in CO_2-C fluxes was observed until day 16, where a second peak on CO_2 flux is observed after turning the piles on composting day 15 (Figure 9a). This peak was significantly higher in the ctrl 8040.6 mg CO_2-C m^{-2} h^{-1} than in the bc treatment (6122.3 mg CO_2-C m^{-2} h^{-1}) (Figure 9a). Subsequently, emissions decreased gradually again. After the second pile turning on day 41 (within mesophilic phase II), CO_2 flux detected on day 42 slightly increased in both crtl (1389.6 mg CO_2-C m^{-2} h^{-1}) and bc (1068.0 mg CO_2-C m^{-2} h^{-1}) compared to the previous measurement, without statistical difference between ctrl and bc (Figure 9a). Towards the later stages of the mesophilic II and maturation phases, CO_2 flux stabilized and reached ambient levels with final values of 28.7 and 21.6 mg CO_2-C m^{-2} h^{-1} in the ctrl and bc treatments, respectively (Figure 9a). Overall, no significant differences were found between the two treatments, except on day 16.

Methane emissions in ctrl and bc mostly occurred within the thermophilic phase and beginning of mesophilic phase II (Figure 9b). A pattern with two peaks was observed, characterized by an initial increase followed by a decrease in emissions during the thermophilic phase and increased emissions after the first pile turning on day 15 (Figure 9b). Overall, treatments showed similar patterns of CH_4 flux over the experiment with emission peaks tending to be higher in bc treatment. In the bc treatment, CH_4 emissions peaked at 7944.2 µg CH_4-C m^{-2} h^{-1} (190.6 mg CH_4-C m^{-2} day^{-1}) on day 19, shortly after the first pile turning, while in the ctrl CH_4 emissions peaked at 4883.2 µg CH_4-C m^{-2} h^{-1} (117.2 mg CH_4-C m^{-2} day^{-1}) on day five (Figure 9b). Throughout the mesophilic phase, CH_4 emissions decreased over time (Figure 9b). From day 58 of composting, no significant CH_4 fluxes were detected using gas chromatography, suggesting the absence of CH_4 emissions beyond this point in the composting process (Figure 9b).

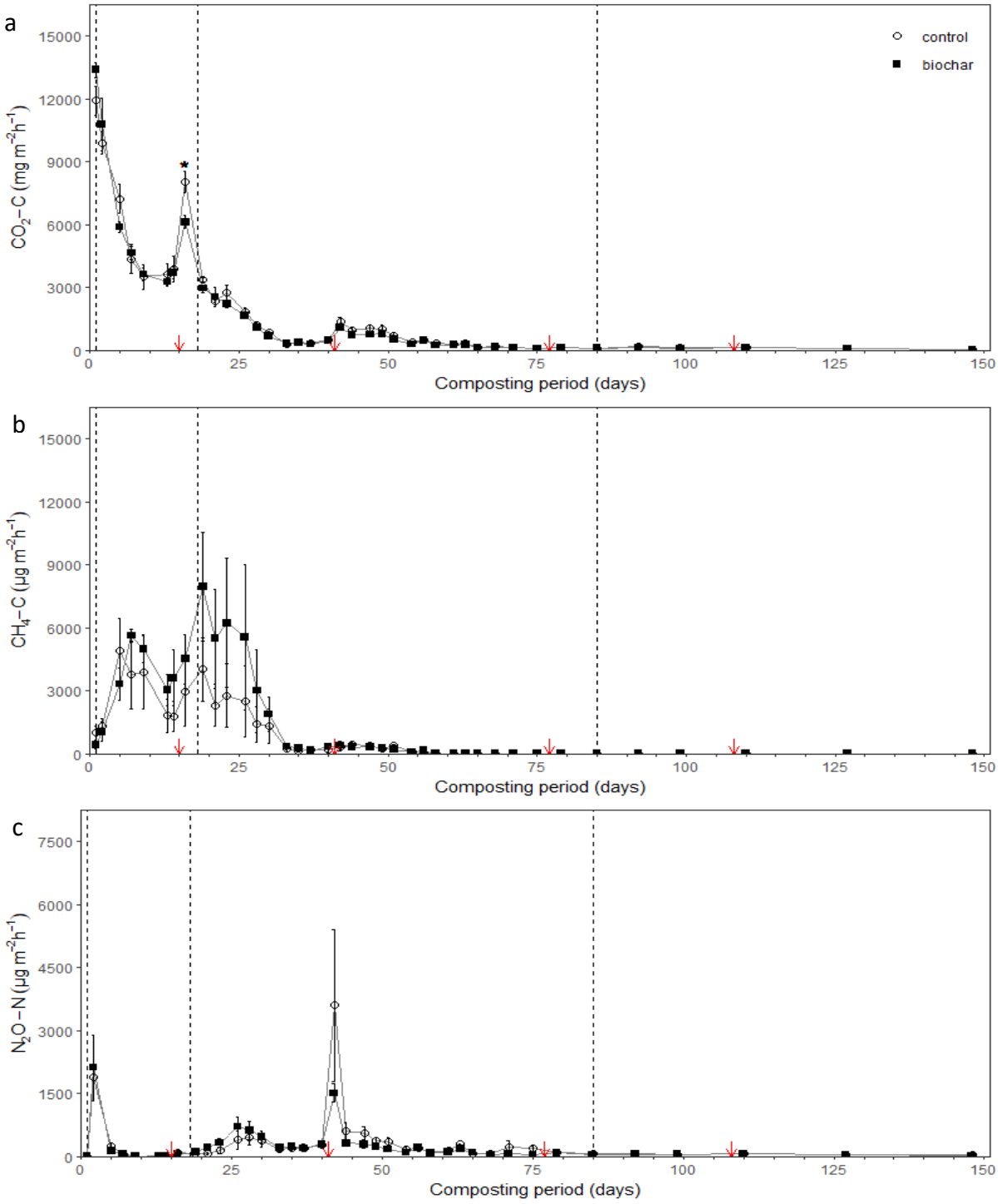

Figure 9 *Dynamics of greenhouse gas emissions during the composting process. a) CO_2-C b) CH_4-C, c) N_2O-N. Values are reported as mean ± SE (n=3). Red arrows indicate turning of the compost piles. Dashed lines indicate compost phases. In figure "a" asterisks (*) indicate significant ($p<0.05$) difference between treatments.*

In both ctrl and bc treatments, N_2O emissions during composting show a bimodal distribution, with a peak at the beginning of the thermophilic phase (day 2) and another peak during the mesophilic phase II (day 42), right after pile turning (Figure 9c). On the second day of composting, N_2O fluxes increased to 1878.4 and 2113.7 µg N_2O-N m^{-2} h^{-1} in the ctrl and bc treatments, respectively (Figure 9c). This was followed by an abrupt decrease of fluxes in both treatments until the end of the thermophilic phase (day 14) (Figure 9c). After the first pile turning on day 15 and with the onset of lower temperatures in the mesophilic phase, emissions increased again similarly in both treatments (Figure 9c). The second peak of N_2O flux occurred after the second pile turning on day 42 with values of 3595.1 µg N_2O -N m^{-2} h^{-1} (86.28 mg N_2O-N m^{-2} day^{-1}) in the ctrl and 1504.4 µg N_2O -N m^{-2} h^{-1} (36.11 mg N_2O-N m^{-2} day^{-1}) in the bc treatment (Figure 9c). Despite the substantial difference in the average N_2O flux on this day, treatments did not differ statistically likely due to heterogeneity of fluxes detected in compost boxes within treatment. Subsequently, emissions decreased during the mesophilic phase II and approached ambient air concentrations during the maturation phase (Figure 9c). The third (day 77) and fourth (day 108) pile turning had no effect on N_2O emissions (Figure 9c).

3.7.2 Cumulative CO_2, CH_4 and N_2O emissions

Cumulative CO_2 emissions averaged at 4015.7 and 3705.8 g CO_2-C m^{-2} in the ctrl and bc treatments, respectively (Figure 10a). This indicates that bc reduced cumulative CO_2-C emissions by 8% compared to ctrl, but this was not confirmed statistically. After day 16, a tendency towards higher cumulative CO_2 emissions in the crtl treatment can be seen, which coincides with the higher fluxes measured after the first turning (Figure 10a).

In the ctrl and bc treatments, cumulative CH_4 emissions averaged 2170.5 and 3332.2 mg CH_4-C m^{-2}, respectively (Figure 10b). These results indicate that the cumulative CH_4-C emission in the ctrl was approximately 34.9% lower compared to bc (Figure 10b). However, it is important to note that the data also showed a considerable degree of variability (Figure 10b). Consequently, statistical analysis did not reveal a significant difference between the two treatments.

Cumulative N_2O emissions averaged 715.1 and 562.8 mg N_2O-N m^{-2} in the ctrl and bc treatment, respectively (Figure 10c). The shift from slightly higher N_2O emissions in the bc treatment towards higher emissions in the ctrl compost after the second turning can be seen clearly (Figure 10c). The results indicate that cumulative N_2O emission in the bc treatment was approximately 21.3% lower compared to the ctrl. Nevertheless, this was not statistically significant.

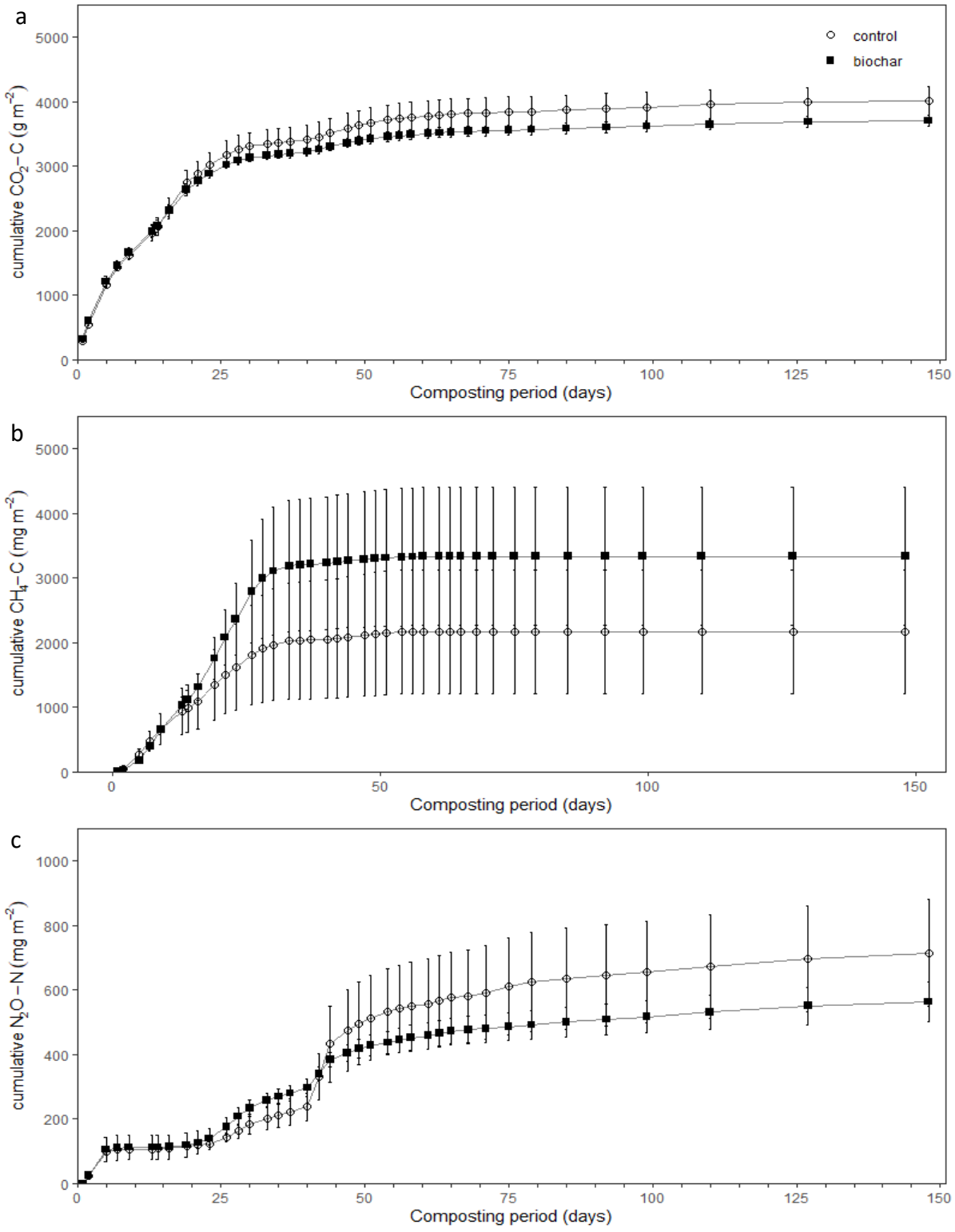

Figure 10 *Cumulative greenhouse gas emissions during composting process with and without (control) biochar. a) CO_2-C, b) CH_4-C, c) N_2O-N. All values are reported as mean ±SE (n=3).*

3.7.3 Global warming potential

In course of the composting the total GHG emissions amounted 4119.0 and 3803.6 g CO_2-C eq m^{-2} in the ctrl and bc treatment, respectively (Figure 11). The contribution of CO_2-C to the GWP was 97.5% in the ctrl and 97.4% in the bc treatment. Although GWP was 7.7% lower in the bc compared to ctrl, this difference was not significant.

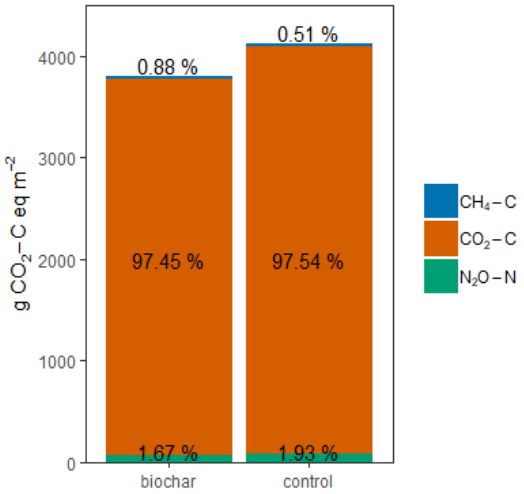

Figure 11 *Global warming potential of the greenhouse gas emissions during the whole composting period expressed in CO_2-C equivalents. Data is reported as mean (n=3).*

3.8 Compost maturation

Results of the GI test conducted with cress seeds on days 104, 126, and 139 of composting are displayed in Table 6. The GI values recorded on days 104 and 126 indicated insufficient maturity of compost in both ctrl and bc treatments (Table 6). It is important to note that using "Sperli Bio" cress the germination rate in the control with distilled water was lower compared to that of "Kiepenkerl" cress. Consequently, one must exercise caution when interpreting these particular values. However, on day 139, the GI values of 0.71 (ctrl) and 0.97 (bc) surpassed the threshold of 0.5, indicating compost maturity (Table 6).

Table 6 *Compost maturity indicators on composting days 104, 126, 139 and 148. Values are reported as mean±SE (n=3).*

	Day 104		Day 126		Day 139		Day 148	
	ctrl	bc	ctrl	bc	ctrl	bc	ctrl	bc
GI (%)	0.11±0.01	0.02±0.03	0.15±0.01	0.17±0.2	0.71±0.14	0.97	-*	-*
EC (mS cm^{-1})	3.1±0.1	2.3±0.1	3.6±0.2	2.8±0.1	3.8±0.1	3.2±0.1	3.5±0.1	2.9±0.1
NH_4^+–N:NO_3^-–N	0.24±0.07	0.17±0.01	0.15±0.02	0.12±0	0.13±0.30	0.07±0.01	0.12±0.01	0.11
NH_4^+–N (mg kg^{-1})	45.6±11.4	31.4±1.7	37.2±7.9	29.9±2.5	32.5±7.3	20.4±2.4	31.5±3.3	29.0±6.7
C:N	12.4±0.2	23.8±0.9	11.9±0.3	22.6±1.3	12.0±0.4	21.7±0.7	11.1±0.4	24.0±1.6
pH	8.9	9.1	8.9±0.1	8.9	8.9±0.1	8.8	8.8±0.1	8.9

*composts were already considered mature based on the previous GI test.

At the end of the composting process, the C:N ratio of compost in ctrl treatment was 11.1 (Table 6), which is within the recommended range. In the bc treatment, the C:N ratio in the final compost was 24.0 likely due to the recalcitrance of bc to degradation (Table 6). The rate of CO_2 production was low during the maturation phase and below 120 mg CO_2 kg^{-1} h^{-1} in both treatments, supporting the GI results indicating compost maturity in both treatments (Figure 9a). This is corroborated by a NH_4^+–N:NO_3^-–N ratio of 0.12 in the ctrl and 0.11 in the bc treatment (Table 6), which are below the maximum threshold of 0.16 used to identify compost maturity. Furthermore, the concentration of NH_4^+–N was also below 0.4 g kg^{-1} in both treatments. Compost temperature in both treatments was stable and close to ambient temperatures. Compost pH was still high but was considered to be stabilized. The EC values also stabilized towards the end of the maturation phase and were in the range of 2–3.5 mS cm^{-1} in the final compost (Table 6). Taking these parameters into account, the compost was classified as mature on day 148.

4. Discussion

4.1 Composting phases and control parameters

4.1.1 Compost phases indicated by temperature

The compost temperature in the two treatments show the typical dynamics of the four phases involved in the proper composting process (Rynk et al., 1992; Román et al., 2015). The initial phase is characterized by a rapid increase in temperature, accompanied by high maximum values, which means that the composition and C:N ratio of the initial feedstock mixture was suitable and allowed an intense microbial activity. This indicates that the easily degradable C-rich materials were rapidly degraded by microorganisms, resulting in the generation of heat (Fischer & Glaser, 2012).

The hygienization phase, which occurred during the thermophilic phase, lasted for 8 days in both treatments. This duration meets the requirements of the German Biowaste Ordinance (Bioabfallverordnung BIOAbfV). This regulation requires that in thermophilic composting, temperatures of at least 55°C must be maintained for a continuous period of two weeks, or temperatures of 60°C for six days or 65°C for three days throughout the composting material to ensure hygienization (Bundesministerium der Justiz und für Verbraucherschutz, 2022). As a result, the final compost is expected to be free of phytotoxic substances and pathogens, making it suitable for improving soil fertility (Bernal et al., 2009).

Several studies have shown that the addition of bc to compost can accelerate composting by altering the environmental conditions within the compost pile and increasing microbial activity (Sánchez-Monedero et al., 2018). This increase in microbial activity is reflected in significantly higher temperatures during the thermophilic phase (Steiner et al., 2010; Kammann et al., 2016; Awasthi et al., 2017; Castro-Herrera et al., 2021). It has also been observed that peak temperatures were reached faster and the thermophilic phase was prolonged in compost amended with bc (Li et al., 2015; Chen et al., 2017). Czekała et al. (2016) observed a shortening of the thermophilic phase and higher temperatures due to the addition of bc, which was explained by an acceleration of OM decomposition. The aforementioned observations, however, were not evident in the present experiment. Although the initial temperature rise to peak values was slightly higher in the bc-amended compost, no significant difference was observed between the treatments. Similar results were reported by Castro-Herrera et al. (2021) in a study investigating the composting of human excreta and cattle manure with bc amendment, where no significant temperature difference was observed during the thermophilic phase in the human excreta compost with and without bc.

4.1.2 Moisture content

Compost MC decreased gradually and sharply until beginning of mesophilic phase II. In particular, the thermophilic phase, characterized by elevated temperatures, showed the highest rate of moisture reduction. Afterwards, watering measures were efficient to prevent piles from drying out below adequate moisture. Previous research has found significantly lower MC in bc-amended compost compared to ctrl, attributed to the addition of bc as a dry bulking agent (Liu et al., 2017; Castro-Herrera et al., 2021). However, the addition of bc was also found to enhance the water retention capacity of the compost substrate due to its porous structure

(Prost et al., 2013; López-Cano et al., 2016). In the present study ctrl and bc exhibited same MC throughout the whole composting period, therefore it is not clear if bc acted as a dry bulking agent or moisture retention agent.

4.1.3 pH and EC

A steady decrease in pH was observed throughout the composting process. The initial pH values of 9.5 in our experiment were found to be higher than those observed in similar studies (Li et al., 2015; López-Cano et al., 2016; Wang et al., 2018; Castro-Herrera et al., 2021). These elevated pH values (>8.5) might have promoted the conversion of NH_4^+ into NH_3, as suggested by Rynk et al. (1992). Therefore, the preferred pH range is 6.5–8, but due to the flexibility of microorganisms to cope with different pH regimes, composting can also take proceed at pH 5.5 or 9 (Rynk et al., 1992). However, previous research reported an initial increase in pH due to the process of ammonification during the thermophilic phase (Rynk et al., 1992; Román et al., 2015; Castro-Herrera et al., 2021), which was not verified in the present experiment. In the course of the composting, the decrease of pH in both ctrl and bc might be associated to the release of H^+ in the nitrification processes, or less likely, to leaching of cations (Sánchez-Monedero et al., 2001), as compost boxes were most of the time covered and leaching was only sporadically observed.

Previous studies have found that the addition of biochar significantly increases the pH of compost (Li et al., 2015; Wang et al., 2018; Castro-Herrera et al., 2021). However, in the present experiment, we did not observe a significant effect of bc on compost pH. Compared to the study of Castro-Herrera et al. (2021), the pH of the bc used in this experiment (8.5) was less alkaline compared to the bc used in their study (10.67). Furthermore, the initial pH of ctrl compost was already 9.5. These observations may explain the similar pH of both treatments during composting and the difference to other studies.

The increase in compost EC over the course of composting can be attributed to several factors, including the mineralization of nutrients contained in OM and increased nitrification. As the OM decomposes, soluble salts are released, thereby increasing compost EC (Maheshwari et al., 2014). Biochar might reduce the concentration of soluble salts by retaining great amounts of nutrients. In addition, the greater loss of compost mass observed in the ctrl throughout the composting process can contribute to higher nutrient concentrations and consequently higher EC values in the compost (Li et al., 2015). The reduction in EC during mesophilic phase II may be related to uncontrolled nutrient leaching after rain entered the compost piles. Despite the increase in compost EC in both treatments over time, the EC of the mature composts was below a threshold of 4 mS cm^{-1}, indicating that ctrl and bc compost are not expected to inhibit plant growth (Lasaridi et al., 2006).

4.1.4 C:N ratio

Based on Rynk et al. (1992), the C:N ratio of the initial compost (24) was close to the ideal range of 25–30. Also, this C:N ratio fell within the wider range of 20–40, which ensures a balanced nutrient composition and favourable conditions for effective composting. Together with the high moisture and high compost and ambient air temperature prevailing in this study in the first weeks of composting, this may have led to fast decomposition of easily degradable organic components of the compost and reduction of compost C:N ratio. This is particularly

seen in the ctrl treatment. During this phase, labile organic compounds, such as carbohydrates, fats and amino acids present in the initial feedstocks, are rapidly degraded (Bernal et al., 2009). As the availability of easily degradable components in the ctrl compost decreased, the C:N ratio reached a more stable level towards the mesophilic phase II and maturation phase.

In the bc treatment, the drop of compost C:N ratio with composting time is affected by the C:N ratio of the bc and its stability during composting. Consequently, the C:N ratio in the bc treatment was significantly higher from day 29 until the end of composting. Here the C:N ratio of the final ctrl compost was in the ideal range of mature compost, whereas that of bc treatment was higher than recommended (Bernal et al., 2009). Similar effects of bc on the C:N ratio of compost were reported in Khan et al. (2014) and Castro-Herrera et al. (2021). It should be noted that bc compost may be characterized by a slower N release rate when applied to soils, which needs to be taken into account when calculating the amount of compost to be applied in order to meet crop N demands (Castro-Herrera et al., 2021).

4.2 TOM, TOC and TN dynamics

The OC content of the substrate decreased during the active phase of composting as a result of microbial decomposition of the OM (Bernal et al., 2009). Correspondingly, a similar dynamic was observed for the dynamics of TOC concentrations compared to TOM degradation in ctrl compost. In the thermophilic phase, there was a rapid decline in OM. This decrease was mainly due to the initial rapid decomposition of easily degradable compounds, facilitated by a favourable C:N ratio (Rynk et al., 1992). As the composting process progresses to the maturation phase and the degradable organic substrates are depleted, the OM undergoes a process of stabilization and humification and the rate of decomposition decreases as the availability of C sources decreases (Bernal et al., 2009; Fischer & Glaser, 2012). As a result, the final compost matures and becomes humic in its OM composition (Bernal et al., 2009; Antunes et al., 2019). The decomposition of OM during the composting process resulted in a decrease in the dry weight of the pile and a reduction in the C:N ratio.

However, when bc is added to the compost, the rate of decomposition of overall OM in the compost was significantly reduced. Our findings of a lower decline in TOM content in bc compared to ctrl are inconsistent with previous studies showing opposite results (Dias et al., 2010; Li et al., 2015). Increased OM decomposition and humification in bc-amended compost in these studies is attributed to bc-induced microbial growth and activity, resulting from improved environmental conditions within the compost pile promoted by bc (Sánchez-Monedero et al., 2018). Possibly, the use of wheat straw in both treatments to increase pile-internal aeration and oxygenation already provided good environmental conditions for OM decomposition, without additional benefits of bc in this respect. The high inherent recalcitrance and aromaticity of the bc used in the present study (as showed by its low H/C = 0.17 and O/C = 0.03 molar ratios, and confirmed by ^{13}C-NMR) is likely less susceptible to microbial degradation during composting (Fischer & Glaser, 2012; Hagemann et al., 2018). Consequently, this may have led to a higher TOC content in the bc compared to the ctrl treatment. In the course of the composting, the TOC content in the bc compost increased because of a concentration effect due to mass loss. While the rest of the composting material was decomposing, the bc remained very stable, as confirmed by temporal ^{13}C NMR analysis of bc particles

picked from the compost. As a result of the mass loss of the composting material, TN content increased over time. Due to a higher mass loss in the ctrl treatment, the final ctrl compost contained significantly higher TN content.

The calculation of nutrient losses showed negative values for N, indicating a N gain during the composting process. These values are somewhat misleading and suggest that the measurements on the first day of sampling may have underestimated the TN content, possibly due to the very heterogenous substrate containing large feedstock pieces (mainly VS). It is also possible that the calculation of the theoretical compost weight, when only OM is taken into account, is not very accurate.

4.3 P and K dynamics

The concentration of P_{av} and K_{av} increased during composting. The decomposition of OM by microorganisms converts complex, bound organic forms into more soluble and plant-available forms (Bernal et al., 2009). A decrease in P_{av} and K_{av} concentrations towards the end of composting, attributed to a shift to more stable P and K forms (Castro-Herrera et al., 2021), was not observed in the present experiment. The similar contents of P_{av} and K_{av} observed in ctrl and bc treatments suggest that immobilization or retention processes of P_{av} and K_{av} by bc were not evident. In co-composting, bc can retain K^+ because the carboxyl groups and the sorbed OM on the bc surface act as sorption sites for K^+ (Prost et al., 2013; Kammann et al., 2016; Wang et al., 2019). This is not evident in the present study as no relevant enrichment of bc with carboxyl C groups due to co-composting was revealed by ^{13}C NMR analysis. However, it is possible that the existing carboxyl C groups acted as sorption sites.

Due to the high levels of Ca^{2+} and Mg^{2+} in bc ash, bc also has a sorption capacity for P in aqueous solution and could reduce P_{av} due to the formation of Mg/Ca phosphate complexes (Wang et al., 2015). Even though the bc used contained Ca^{2+} and Mg^{2+} in the ash, no significant reduction in P_{av} content was not observed in the bc compost.
Also the presence of tightly bound phosphates in the organo-mineral layer of the bc or precipitates on the positively charged minerals on the bc surface or in the pores (Kammann et al., 2015; Joseph et al., 2018), were not evident in the present study.

4.4 Nitrogen dynamics

During the decomposition of OM, N in organic compounds is initially released in the form of NH_4^+ which is reflected in the high amounts measured at the beginning of the composting in both treatments. The subsequent decrease in NH_4^+ concentration can be attributed to N transformation processes explained before (Bernal et al., 2009). In this experiment the rapid decline in NH_4^+ concentration during the thermophilic phase is likely due to the loss of NH_3 by volatilization because the high compost pH values (>9) and elevated temperatures (>45°C) favour this process (Rynk et al., 1992; Beck-Friis et al., 2001; Bernal et al., 2009). However, the extent of NH_3 losses could not be quantified due to methodological constraints.
Nitrification began when temperatures dropped below 45°C, which favours establishment or reactivation of nitrifying bacteria in the compost (Sánchez-Monedero et al., 2001). As the nitrification process takes place under aerobic conditions, turning the compost resulted in increased NO_2^-–N concentrations. A significant impact due to the addition of bc could not be found. In contrast to other studies, no significant effect of bc on N_{min} dynamics in compost

could be demonstrated (Hagemann et al., 2017; Castro-Herrera et al., 2021). A trend towards higher NH_4^+–N (mg kg^{-1}) in the ctrl compost can be observed, indicating a possible retention on the bc surface due to the mechanisms explained before. A reduced concentration of extractable NO_3^- due to bc amendment could not be found which is similar to the findings of Agyarko-Mintah et al. (2017). Studies that found a reduction of NO_3^- in the compost substrate attributed this reduction to the above-mentioned retention mechanisms (Hagemann et al., 2017b; Joseph et al., 2018). In the present study, the final concentrations of NO_3^-–N (mg kg^{-1}) were not statistically different. However, the amount of NO_3^-–N (g $pile^{-1}$) in the whole compost pile is significantly higher in the bc treatment compared to the ctrl. This finding is very important as it shows that when more substrate is added to the compost with bc, there is no dilution of NO_3^-–N concentrations in the final compost. Rather, the bc prevented NO_3^-–N from being lost through the retention mechanisms that will be discussed in more detail in the following section.
The chosen extraction method, using 0.01 mol L^{-1} $CaCl_2$, extracted the soluble N_{min} which represents an approximation of the condition in the soil solution.

4.5 N forms and amounts retained in biochar particles during composting

Conclusions about N_{min} dynamics and availability in the compost substrate as affected by N retention in bc particles should be drawn with caution, as no N_{min} extraction with 2 M KCl was performed for the compost substrate as for the bc particles. Without this extraction, it is difficult to determine if all of the N_{min} not extracted by 0.01 mol L^{-1} $CaCl_2$ is actually bound to the bc surface or if there is additional N_{min} in the compost substrate of both treatments that is immobilized and unavailable to plants. Nevertheless, a similar temporal dynamic can be observed when comparing the N_{min} bound to the bc and that extracted from the compost substrate samples.

In the early stages of composting, freshly added bc showed a high sorption capacity, allowing it to retain a large amount of NH_4^+–N. In the this composting phase, the organic N is mineralized and can bind to the functional groups on the bc surface (Le Leuch & Bandosz, 2007). Here, other mechanisms of NH_4^+–N capture by bc could be considered, as the fresh bc was poorly functionalized (e.g., with carboxylic groups), as evidenced by ^{13}C NMR. Most of the NH_4^+–N retained by bc within the first week of composting was water-extractable and released in the ongoing compost process. This reduction can be attributed to the conversion of easily available NH_4^+–N into other forms of N during the composting process. Consequently, the concentration of easily extractable NH_4^+–N decreased over time, while that of tightly bound NH_4^+–N to bc remained practically unchanged. It can also be assumed that the bc particles not only absorbed N-forms (NH_4^+–N, NO_2^-–N and NO_3^-–N) through the composting process, but that conversion processes also took place on the bc surface. The ferric oxides measured in the bc ash could have led to further redox reactions and hence oxidation of NH_4^+ to NO_3^- at the surface (Li et al., 2012). This may be the reason why only small amounts of NO_3^-–N were measured in the compost samples on day 48, whereas higher amounts of NO_3^-–N could be extracted from the bc particles. It could also have caused the slightly higher NO_3^-–N concentrations in the bc treatment compared to the ctrl on day 57. After the second turning, which was characterized by a clear NO_2^-–N increase in the bc compost, the concentrations of NH_4^+–N that could be extracted with water from bc particles decreased. It is plausible that the bc-

retained NH_4^+–N was used as an additional N source for conversion (into NO_2^-) during this period. It is noticeable that the concentrations of plant-available NH_4^+–N tended to be higher in the ctrl compost. This observation can be explained by both the concentration effect resulting from higher mass loss and the binding of NH_4^+–N to bc particles (less in easily available and more in strongly retained manners). From the beginning of composting, the content of highly bound NH_4^+–N on the bc surface was quantified using a long-term shaking method and showed an increase in concentration.

Although no significant lower NO_3^-–N concentrations were measured in the bc compost compared to the ctrl, a amount of up to 194 mg kg^{-1} NO_3^-–N was strongly retained in the bc particles. This suggests that bc has a remarkable capacity to retain and sequester NO_3^-, functioning as an extra N reservoir during composting. During the composting process, the amount of retained NO_3^-–N, particularly in the form of tightly bound NO_3^-–N, increased. This retention of NO_3^-–N by bc involves complex binding mechanisms that have been investigated in previous studies. In this study the binding mechanism could not be examined in detail. There are several processes that have been found to bind anions to bc. NO_3^- might be bound to the bc particles or form a coating of OM on the surface (Hagemann et al., 2017b; Joseph et al., 2018). During the co-composting of bc, nutrient-rich water can enter the pores and, by partially closing the meso- and macropores, result in NO_3^- being trapped in the micropores (Joseph et al., 2018). There also may be indirect positive binding sites in dissolved organic C, which may not be tightly bound to the composted bc (Kammann et al., 2015; Joseph et al., 2018). In the present study, an indicator of direct sorption sites can be the presence of iron(III) oxides (Fe_2O_3) or manganese (IV) oxide (MnO_2) in the bc we used (Appendix: Table A.1)

Due to the complexity of the binding mechanisms and the varying redox environments, different biotic and abiotic reactions can take place, resulting in nitrification and denitrification (Joseph et al., 2018). As a result, an increase in the concentration of NO_3^-–N from bc was observed during composting. The bonding was weak and strong, which could also be shown by our three extraction steps. Specifically, a significant amount of strongly bound (247.8 mg kg^{-1}) of NO_3^-–N (calculated as the sum of extraction steps 2 and 3) was stored in bc in the final compost. In addition, readily available or weakly bound (first extraction step) NO_3^-–N (164.4 mg kg^{-1}) could be extracted from the bc particles in the final compost, which can be taken up by plants but is also at risk of leaching. Total plant available N, which includes the sum of NH_4^+–N and NO_3^-–N retained in bc, was found to be lower at 172.8 mg kg^{-1} (extracted with water) compared to both the ctrl compost (287.6 mg kg^{-1}) and the bc compost (290.5 mg kg^{-1}). The strongly bound NO_3^-–N in the bc can be considered as a NO_3^- stock and is possibly protected from leaching after the application to soils. However, soil chemical processes could remobilize this stored NO_3^- (Haider et al., 2020).

Our findings are consistent with previous studies which investigated field-aged or co-composted bc with repeated extraction methods (Kammann et al., 2015; Haider et al., 2016; Hagemann et al., 2017a). These studies showed that while some N_{min} can be rapidly extracted from bc particles, a larger proportion remains trapped and requires subsequent extraction steps to be released. Haider et al. (2016) found that the standard extraction method (2 M KCl) only extracted 13% of the total amount of NO_3^- extracted after 10 repeated extractions from field-aged bc. In the field this observation caused a significant NO_3^- retention in the topsoil

with slow NO_3^- release mechanisms (Haider et al., 2016). This slow release of N might act as a protective measure, preventing excessive leaching flush. However, it is worth noting that the use of co-composted bc alone may still be beneficial for plant nutrition as N is retained not only in a tightly bound form that is not only resistant to loss but also partially available for prompt plant uptake. Kammann et al. (2015) showed that the application of co-composted bc particles to the soil resulted in a significantly greater improvement in plant growth compared to raw bc. This effect is probably attributed to the enriched nutrient content, particularly the higher NO_3^- levels. In a subsequent study conducted by Haider et al. (2020), they investigated the impact of naturally field-aged bc on quinoa and perennial ryegrass. Their hypothesis that some of the NO_3^- bound by the bc would remain unavailable and could be extracted after repeated extraction after the experiment was refuted, as the N uptake by quinoa was significantly higher (120%) when N was provided from aged bc compared to synthetic N application (Haider 2020). This finding indicates that N retained in the bc was just as plant-available as mineral fertilizer-derived NO_3^-, proving its potential to enhance N use efficiency in agriculture and suggesting a sustainable option to improve agricultural productivity (Haider et al., 2020).

4.6 Changes in the chemical structure of aged biochar and implications for compost parameters and nutrient retention

The high aromaticity and low functionality of OriBc, Bc77 and Bc148 biochars are typical of woody feedstock-derived bc produced at high pyrolysis temperatures (as described in section 1.2.2) (Cao et al., 2012). Despite the consistent reduction of bc aromaticity with aging, the ^{13}C-NMR spectra revealed incipient functionalization of bc structure (e.g., enrichment with carboxyl C). According to Hilscher and Knicker (2011), the oxidation of aryl C structure occurs in two steps, first aromatic C is modified microbiologically by substitution with OH-groups to form catechol-like compounds, followed by cleavage of O-aryl C rings leading to enrichment in carboxyl C groups. In fact, this is evidenced by the gradual increase of the ratio carboxyl C + O/N-aryl C/aryl C with aging: OriBc (0.12), Bc77 (0.13), Bc148 (0.15). However, these chemical shifts were still minimal evidencing that bc aging and functionalization is incipient after 148 days of co-composting. This is probably associated to the high aromaticity of the bc used in the experiment, which enhances its resistance against biodegradation (Wang et al., 2022). In the present study, the clear reduction in bc aromaticity is attributed to enrichment in alkyl C forms with aging rather than to carboxylic groups formation. The magnitude of chemical shifts in the bc with aging found in the present study are quite similar to that reported by De la Rosa et al. (2018) for sewage-sludge derived bc produced at 600°C and aged in soil for 120 days. The authors observed that aging of bc reduced the aryl C signal from 58 to 51% and increased the alkyl C signal from 7 to 12%. According to the authors, this was caused by fungi colonization of bc pores leading to increase in alkyl C forms and degradation of aromatic structures of the bc by the fungi. Consequently, the authors found that the aromaticity index of the original bc was 1.8-fold greater compared to the aged bc, which is comparable to value found in the present study (1.7-fold) when comparing OriBc and Bc148. Furthermore, the authors observed minimal carboxyl C enrichment in bc after aging (1%), as similarly found in the present study (0.8%).

The high C:N ratio of the original bc along with the chemical stability of the bc against biodegradation via co-composting (as verified by ^{13}C NMR) may explain the persistently higher C:N

ratio, pile weight, TOC (%) and TOM (%) in the bc treatment compared to the ctrl. Also, the accentuated predominance of highly stable C forms in the original and aged bc, likely prevented relevant bc-derived CO_2 emission contributions to the cumulative CO_2-C emissions in bc. Based the feedstock and pyrolysis temperature used for bc production and on the ^{13}C NMR spectra of the bc, it is assumed that its cation exchange capacity was low and kept mostly unaltered along the composting period. Nevertheless, it may still help to explain NH_4^+ retention in bc particles throughout the composting process, as bc surfaces are predominantly negatively charged. The minimal enrichment in carboxyl C after bc aging indicates that increased capture of NO_3^-–N by bc particles across composting days may likely occur by other mechanisms rather than by cation bridges between bc carboxylic groups and NO_3^-. The high BET surface area of the bc used in the present thesis (421 m^2 kg^{-1},Table 3) together with the MC of the compost pile (mostly between 50–70%) may have favoured the transport of NO_3^- with water towards internal bc pores (Hageman et al., 2017a). This is in line with Hageman et al. (2017a), who found greater NO_3^- in co-composted bc with greater BET surface area. Entrapment of NO_3^- in bc pores may have been facilitated by organic coating of bc due to bc particles contact with compost, which reduce the hydrophobicity of bc (Hageman et al., 2017b). In the present work this is supported by a gradual reduction of the hydrophobicity index of bc with aging, as follows: OriBc (22.2), Bc77 (17.5), Bc148 (15.7). Furthermore, NO_3^- may also adhere to the organic coating formed on bc surfaces (Harter et al., 2016; Haider et al., 2020).

4.7 GHG emissions

4.7.1 Temporal and cumulative CO_2 emissions

The CO_2 fluxes observed in ctrl and bc treatment during composting with high initial CO_2 emissions are typically produced due to mineralization and metabolism of simple organic C components by microorganisms during aerobic decomposition (Bernal et al., 2009; Sánchez et al., 2015). Unlike many previous studies, this study found no significant difference between ctrl and bc treatments regarding CO_2 fluxes (Steiner et al., 2010; Czekała et al., 2016; Awasthi et al., 2017; Castro-Herrera et al., 2023). When composting poultry manure, Czekała et al. (2016) found that the addition of bc increased CO_2 emissions, which was explained by increased decomposition of OM due to better conditions resulting from increased porosity and surface area of the bc amendment. Steiner et al. (2010) reported a 28% increase in CO_2 when 20% bc was added, as bc promoted oxygen availability and growth of the microbial population in the compost. Awasthi et al. (2017) found that CO_2 emissions increased proportionally with the amount of bc added when composting sewage sludge investigated and high doses (>8% bc amendment) increased the rate of CO_2 production, while low doses had significantly lower emissions. Similar observations were made when 3% or 5% bc was added to manure composting, with no significant effect on CO_2 release (Steiner et al., 2010; Sánchez-García et al., 2015). The rate of bc applied to the compost in this study (15%) was below the upper threshold of 20% (Sánchez-Monedero et al., 2018), and the observations for CO_2 flux were similar to studies with lower application rates, confirming that rates below 20% tend to prevent additional CO_2 flux from bc-amended compost. However, the observations of no higher CO_2 fluxes might be related to the lower degradation rates of OM and organic carbon in the bc treatment. After the first pile turning, significantly higher CO_2 emissions are observed in the ctrl compost and this is consistent with a more pronounced decrease of OM in the ctrl compared to the bc

treatment. Overall, this study revealed similar CO_2 fluxes in ctrl and bc treatment, suggesting that the application of 15% of the selected bc likely did not alter compost pile oxygenation or microbial activity substantially, as well as it did not cause additional CO_2 emissions.

4.4.2 Temporal and cumulative CH_4 emissions

As explained before, large amounts of CH_4 can occur when anaerobic microsites can occasionally develop in the piles (Rynk et al., 1992). Due to the high oxygen consumption of microbial degradation of easy available organic compounds and the stimulation of microbial growth, O_2 levels can deplete and anaerobic patches can develop (Sonoki et al., 2013; Sánchez-García et al., 2015), leading to CH_4 production as result of the anaerobic decomposition of organic compounds by methanogenic organisms (Sonoki et al., 2013). For instance, several studies have found that the addition of bc can significantly reduce CH_4 emissions by increasing compost oxygenation, but this was not shown in our results (Sonoki et al., 2013; Agyarko-Mintah et al., 2017; Chen et al., 2017; Castro-Herrera et al., 2023). It is possible that bc increases the physical structure of the compost substrate through lower bulk density and more micro- and macropores (Agyarko-Mintah et al., 2017; Chen et al., 2017). Sonoki et al. (2013) found that when 10% bc was added to the compost, the level of methanogenic organisms was two times lower than in the ctrl compost, while the level of methanotrophic organisms was three times higher, which was explained by the porous structure of the bc. Agyarko-Mintah et al., (2017) showed that after prolonged periods without compost turning, anaerobic sites can be formed. In the present work, even though 16% WS was used intended to compost aeration and piles were turned 4 times still CH_4 peaks occurred in both ctrl and bc treatments, suggesting the quick formation of anaerobic spots within the compost. However, as CH_4 fluxes in ctrl did not differ from that in bc treatments, it seems that anaerobic patches in the compost were not bc-related. Similarly, Sánchez-García et al. (2015) reported that bc amendment to compost at 3% did not change CH_4 fluxes compared to ctrl because this bc proportion in the compost might not be sufficient to change compost aeration conditions. An indication of anaerobic conditions in the compost piles in the present study could be moist and compact patches observed at the bottom of the compost piles during piles turning, particularly bc treatment. However, the MC was similar in ctrl and bc along composting duration and possible additional anaerobic microsites in bc compost were not picked by MC data.

4.4.3 Temporal and cumulative N_2O emissions

Several studies found significantly lower N_2O emissions when bc was added to compost (Wang et al., 2013; Agyarko-Mintah et al., 2017; Awasthi et al., 2017; Castro-Herrera et al., 2023; Wang et al., 2018). Li et al. (2016) found that bc reduced cumulative N_2O emissions by 54.1% compared to ctrl compost. In the present experiment, bc did not reduce cumulative N_2O emissions, but on the other hand it also did not increase it. Moreover, after the second compost turning the N_2O emission peak was higher in the ctrl compared to bc treatment. It is possible that the N pool available in the compost to nitrifying and denitrifying bacteria that produce N_2O is reduced because bc adsorbs large amounts of NH_4^+ and NO_3^- (Awasthi et al., 2017). This is likely in our study because when high N_2O emissions occurred after the second turn, a significant amount of NH_4^+–N was strongly bound to the bc particles. Therefore, the amount of

available NH_4^+–N that could be oxidized in the bc treatment was lower than in the ctrl compost. It can be assumed that this higher N_2O flux peak in ctrl was due to nitrification, as NO_3^- concentrations also increased after the peak.

The N_2O emissions measured in this experiment were significantly lower than in similar bc composting setups, with peak emissions of 36.1 to 83.3 mg N_2O-N m^{-2} day^{-1} in the present study (Li et al., 2016; Castro Herrera et al., 2023). Castro-Herrera et al. (2023) observed peak emissions of 198–789 mg N_2O m^{-2} day^{-1} on day 34 of composting and cumulative emissions of 6.8–22.7 g N_2O m^{-2} during 143 days of composting. Higher N_2O emissions in Castro Herrera et al. (2023), for example, can be attributed to a different feedstock composition with cattle manure or humanure, vegetable scraps and teff straw. In their study, the initial NH_4^+–N concentrations were 2830 mg kg^{-1} (humanure) and 3428 mg kg^{-1} (cattle manure), which are significantly higher than the concentrations of the raw materials used in this study (VS 205.4 mg kg^{-1}; HM 15.2 mg kg^{-1}). These low NH_4^+–N concentrations are probably reflected in the low N_2O emission data. Li et al. (2016) measured even higher peak emissions of 613.4 - 3567.6 mg N_2O m^{-2} day^{-1} and 28 - 60 g N_2O m^{-2} over a windrow composting period of 65 days with a feedstock of cattle manure and rice straw. Low N_2O emissions were reported by He et al. (2017) were cumulative emissions during 55 days of large-scale composting of fresh pig manure and dry chicken manure ranged from 0.1368 (bc) to 0.3166 (ctrl) g N_2O m^{-2}.

4.8 Global warming potential

Compost emissions of CO_2, CH_4 and N_2O can contribute significantly to global warming, with CH_4 and N_2O having GWP 28 and 265 times greater than CO_2, respectively, over a 100-year time horizon (IPCC, 2013).

In this experiment, the similar CO_2, CH_4 and N_2O fluxes observed in ctrl and bc led to comparable GWP in the two treatments. In a human excreta and cattle manure compost experiment with bc Castro-Herrera et al. (2023) found comparatively higher GWP values than found in this study. Furthermore, the authors detected no significant difference between bc amended and ctrl treatments, as lower CH_4 and N_2O emissions were offset by higher CO_2 emissions in the bc treatment. Our research showed a lower GWP, mainly due to reduced N_2O emissions in both treatments compared to the cited work. Similarly, Wang et al. (2021) observed that the addition of bc did not significantly reduce GWP, probably because CH_4 emissions remained relatively high despite lower N_2O emissions. He et al. (2017) found a significantly lower GWP of 19.82 when using bc powder compared to the ctrl compost. It is important to note that they excluded CO_2 from the GWP analysis, considering it a biogenic source.

4.9 Compost maturity and stability

The final GI values >50% indicated according to Zucconi (1981) compost maturity for both treatments. According to the Compost Maturity Index presented by the Californian Compost Quality Council (CCQC), which is often used to classify compost maturity and stability, compost is very mature (GI>90%), mature (GI 80–90%) and immature (GI<80%) (CCQC., 2001). Based on this GI ranking, ctrl compost was classified as mature and bc compost as very mature. The GI values in the present experiment are lower after 148 days than in Castro-Herrera et al. (2021) with GI>100% after 183 days or Li et al. (2016) with >100% after 90 days.

The C:N values in the ctrl compost were in the ideal range <20 for mature compost. Compost with a C:N greater than 25 is considered immature (CCQC). According to the maturity assessment, composts with a C:N ratio equal to or less than 25 must at least meet other parameters of stability (group A) and maturity (group B).
With the CO_2 production rate as an indicator of stability this is met by the bc treatment and the ctrl treatment. In terms of maturity parameters (NH_4^+–N:NO_3^-–N, NH_4^+–N concentrations), both treatments are considered to be very mature.
Similar observations of high C:N values are noticed in other studies and therefore Khan et al. (2014) suggests that also maturity indices, which are independent of recalcitrant C, should also be taken into account if bc is a significant added in a significant amount.

5. Conclusion

A successful composting process was achieved by mixing the initial feedstock of VS, HM and WS, with an initial temperature increase and characteristic pattern of different compost phases observed in the ctrl and bc-amended composts. The high temperatures reached in the thermophilic phase also suggest a hygienization of the feedstock, which is important for the manure treatment. An initial decrease and subsequent stabilization of OM suggest that composting has produced a final nutrient-rich fertilizer without phytotoxic compounds. Contrary to expectations, the addition of bc did not significantly alter the composting process. However, GI in the bc was higher in the bc amended compost.

We found that the addition of bc did not have a negative effect on the temporal dynamics of GHG emissions and no statistically significant difference was observed between the two treatments. Both treatments showed similar patterns in CO_2, CH_4 and N_2O emissions within the composting phases and the levels of peak emissions were not significantly different, except for higher CO_2 emissions in the ctrl compost after the first turning. No significant difference in the cumulative GHG emissions could be observed between both treatments. The GWP was slightly higher for the ctrl compost, but not significantly different.

Contrary to previous studies and our assumption that bc would reduce N_2O emissions, this could not be confirmed on the basis of the measurements carried out. However, a trend towards reduced N_2O emissions in the bc treatment could be observed after turning the piles in mesophilic phase II. The bc compost did not show statistically significant lower emissions compared to the ctrl compost. Therefore, the hypothesis that the temporal dynamics of N_2O emissions is associated to N forms and availability in bc particles cannot be confirmed as we could not see this effect clearly. Based on the observations, only assumptions can be made. We link the trend towards reduced N_2O emissions after turning the compost to the reduced availability of NH_4^+–N in the compost substrate with bc addition. This reduced availability is explained by the retention by bc, since the amount of strongly retained NH_4^+–N was stable even after turning the piles. The retention is therefore interpreted as a reduction in the pool of NH_4^+ that can be transformed. This probably attenuated N_2O emissions after compost turning in the bc treatment compared to the ctrl. Despite the retention of different N forms with a varying degree of strength that was observed, this was not reducing the nitrification rates and N_2O emissions over the entire composting period as we hypothesized. However, the repeated extraction method confirmed the hypotheses that bc retains NH_4^+ and NO_3^- in both available and unavailable forms during the composting of organic residues.

We could not confirm that the functionalization of BC by co-composting contributed to the retention of NH_4^+. 13 CNMR data showed that fresh bc was poorly functionalized and after 148 days of co-composting, bc aging and functionalization were still minimal. Perhaps, but not investigated in this study, NH_4^+ retention due to entering and clogging of soluble OM into the BC pores could be more apparent.

The hypothesis that bc reduces N losses during composting of HM, organic waste and WS can be partially confirmed. The higher levels of NO_3^-–N in the bc compost box suggest that the

addition of bc and the associated retention protected against loss by leaching. Also the retention of NH_4^+–N and no lower concentrations indicate no loss of NH_4^+. A reduced loss due to N_2O emissions could not be statistically confirmed. No conclusions can be drawn about the loss of NH_3 as we were not able to measure these emissions.

However, the long-term stability of the N forms retained when co-composted bc is applied to soils requires further investigation. In this context, it would be interesting to know how plant-available N is under field conditions and if bc application can reduce the use of mineral fertilizer. Therefore, the mechanism of N release needs further investigations, e.g. how different soil types or land management systems influence the release. It is also important to know if the retained and strongly bound N is likely to leach.

In this experiment the feedstock used had low initial NH_4^+–N concentrations. It would be interesting to investigate the retention at higher initial NH_4^+–N concentrations and to see how much N can be retained and if a sorption maximum is reached, how strong these bonds might be.

It is important that further research is conducted to provide scientifically validated results so that the potential use of co-composted bc in agricultural practice leads to sustainable solutions, promotes soil, environmental and climate protection, and ensures food security.

6. References

Abbruzzini, T. F., Davies, C. A., Toledo, F. H., & Cerri, C. E. P. (2019). Dynamic biochar effects on nitrogen use efficiency, crop yield and soil nitrous oxide emissions during a tropical wheat-growing season. *Journal of environmental management,* 252, 109638. https://doi.org/10.1016/j.jenvman.2019.109638

Abelmann, K., Kleineidam, S., Knicker, H., Grathwohl, P., & Kögel-Knabner, I. (2005). Sorption of HOC in soils with carbonaceous contamination: Influence of organic-matter composition. *Journal of Plant Nutrition and Soil Science*, 168 (3), 293-306. https://doi.org/10.1002/jpln.200421622

Agyarko-Mintah, E., Cowie, A., Singh, B. P., Joseph, S., van Zwieten, L., Cowie, A., Harden, S., & Smillie, R. (2017). Biochar increases nitrogen retention and lowers greenhouse gas emissions when added to composting poultry litter. *Waste Management*, 61, 138–149. https://doi.org/10.1016/j.wasman.2016.11.027

Ahn, H. K., Mulbry, W., White, J. W., & Kondrad, S. L. (2011). Pile mixing increases greenhouse gas emissions during composting of dairy manure. *Bioresource Technology*, 102(3), 2904–2909. https://doi.org/10.1016/j.biortech.2010.10.142

Amelung, W., Blume, H.-P., Fleige, H., Horn, R., Kandeler, E., Kögel-Knabner, I., Kretzschmar, R., Stahr, K., & Wilke, B.-M. (2018). Böden als pflanzenstandorte. In Amelung et al. (Ed.), *Scheffer/Schachtschabel Lehrbuch der Bodenkunde 17. Auflage* (pp. 491-581). Springer Nature. https://doi.org/10.1007/978-3-662-55871-3_9

Antunes, R. M., dos Anjos Leal, O., Vargas Castilhos, R. M. Dufech Castilhos, D., Andreazza, R., & Schwalbert, R. A. (2019). Humic Substances and Chemical Properties of an Acrisol Amended with Vermicomposted Vegetal and Animal Residues. Revista Brasileira de Ciência do Solo, 43, *e0180032*. https://doi.org/10.1590/18069657rbcs20180032

Awasthi, M. K., Wang, M., Chen, H., Wang, Q., Zhao, J., Ren, X., Li, D.-S., Awasthi, S. K., Shen, F., Li, R., & Zhang, Z. (2017). Heterogeneity of biochar amendment to improve the carbon and nitrogen sequestration through reduce the greenhouse gases emissions during sewage sludge composting. *Bioresource Technology*, 224, 428–438. https://doi.org/10.1016/j.biortech.2016.11.014

Beck-Friis, B., Pell, M., Sonesson, U., Jönsson, H., & Kirchmann, H. (2000). Formation and Emission of N2O and CH4 from Compost Heaps of Organic Household Waster. *Environmental Monitoring and Assessment*, 62(3), 317–331. https://doi.org/10.1023/A:1006245227491

Beck-Friis, B., Smårs, S., Jönsson, H., & Kirchmann, H. (2001). SE—Structures and Environment. *Journal of Agricultural Engineering Research*, 78(4), 423–430. https://doi.org/10.1006/jaer.2000.0662

Bernal, M. P., Alburquerque, J. A., & Moral, R. (2009). Composting of animal manures and chemical criteria for compost maturity assessment. A review. *Bioresource Technology*, 100(22), 5444–5453. https://doi.org/10.1016/j.biortech.2008.11.027

Borchard, N., Spokas, K., Prost, K., & Siemens, J. (2014). Greenhouse gas production in mixtures of soil with composted and noncomposted biochars is governed by char-associated organic compounds. *Journal of Environmental Quality*, 43(3), 971–979. https://doi.org/10.2134/jeq2013.07.0290

Borchard, N., Schirrmann, M., Cayuela, M. L., Kammann, C., Wrage-Mönnig, N., Estavillo, J. M., Fuertes-Mendizábal, T., Sigua, G., Spokas, K., Ippolito, J. A., & Novak, J. (2019). Biochar, soil and land-use interactions that reduce nitrate leaching and N2O emissions: A meta-analysis. *The Science of the Total Environment*, 651, 2354–2364. https://doi.org/10.1016/j.scitotenv.2018.10.060

Bouwman, L., Goldewijk, K. K., van der Hoek, K. W., Beusen, A. H. W., van Vuuren, D. P., Willems, J., Rufino, M. C., & Stehfest, E. (2013). Exploring global changes in nitrogen and phosphorus cycles in agriculture induced by livestock production over the 1900-2050 period. *Proceedings of the National Academy of Sciences of the United States of America*, 110(52), 20882–20887. https://doi.org/10.1073/pnas.1012878108

Bundesministerium der Justiz und für Verbraucherschutz (2022).Verordnung über die Verwertung von Bioabfällen auf landwirtschaftlich, forstwirtschaftlich und gärtnerisch genutzten Böden (Bioabfallverordnung–BioAbfV): BioAbfV. Bundesministerium der Justiz und für Verbraucherschutz: Bundesministerium der Justiz und für Verbraucherschutz. http://www.gesetze-im-internet.de/bioabfv/index.html

California Compost Quality Council. (2001). *Compost maturity index*. CCQC.

Canadell, J., Monteiro, P., Costa, M., Da Cotrim Cunha, L., Cox, P., Eliseev, A. V., Henson, S., Ishii, M., Jaccard, S., Koven, C., Lohila, A., Patra, P. K., Piao, S., Rogelj, J., Syampungani, S., Zaehle, S., & Zickfeld, K. (2021). Global Carbon and other Biogeochemical Cycles and Feedbacks. In V. Masson-Delmotte (Ed.), *Climate Change 2021: The Physical Science Basis. Contribution of Working Group I to the Sixth Assessment Report of the Intergovernmental Panel on Climate Change*, 673–816. https://doi.org/10.1017/9781009157896.007

Cao, X., Pignatello, J. J., Li, Y., Lattao, C., Chappell, M. A., Chen, N., Miller, L. F., & Mao, J. (2012). Characterization of Wood Chars Produced at Different Temperatures Using Advanced Solid-State 13 C NMR Spectroscopic Techniques. *Energy & Fuels*, 26(9), 5983–5991. https://doi.org/10.1021/ef300947s

Castro-Herrera, D., Prost, K., Schäfer, Y., Kim, D.-G., Yimer, F., Tadesse, M., Gebrehiwot, M., & Brüggemann, N. (2021). Nutrient dynamics during composting of human excreta, cattle manure, and organic waste affected by biochar. *Journal of Environmental Quality*, 51(1), 19–32. https://doi.org/10.1002/jeq2.20312

Castro-Herrera, D., Prost, K., Kim, D.-G., Yimer, F., Tadesse, M., Gebrehiwot, M., & Brüggemann, N. (2023). Biochar addition reduces non-CO2 greenhouse gas emissions during composting of human excreta and cattle manure. *Journal of Environmental Quality*, 52(4), 814-828. https://doi.org/10.1002/jeq2.20482

Cayuela, M. L., van Zwieten, L., Singh, B. P., Jeffery, S., Roig, A., & Sánchez-Monedero, M. A. (2014). Biochar's role in mitigating soil nitrous oxide emissions: A review and meta-analysis. *Agriculture, Ecosystems & Environment*, 191, 5–16. https://doi.org/10.1016/j.agee.2013.10.009

Chen, W., Liao, X., Wu, Y., Liang, J. B., Mi, J., Huang, J., Zhang, H., Wu, Y., Qiao, Z., Li, X., & Wang, Y. (2017). Effects of different types of biochar on methane and ammonia mitigation during layer manure composting. *Waste Management*, 61, 506–515. https://doi.org/10.1016/j.wasman.2017.01.014

Conte, P., & Alonzo, G. (2007). Environmental NMR: fast-field-cycling relaxometry. *eMagRes* 2, 389–398 https://doi.org/10.1002/9780470034590.emrstm1330

Czekała, W., Malińska, K., Cáceres, R., Janczak, D., Dach, J., & Lewicki, A. (2016). Co-composting of poultry manure mixtures amended with biochar - The effect of biochar on temperature and C-CO2 emission. *Bioresource Technology*, 200, 921–927. https://doi.org/10.1016/j.biortech.2015.11.019

De La Rosa, J., Miller, A. Z., & Knicker, H. (2018). Soil-borne fungi challenge the concept of long-term biochemical recalcitrance of pyrochar. *Scientific Reports*, 8(1), 2896. https://doi.org/10.1038/s41598-018-21257-5

Dias, B. O., Silva, C. A., Higashikawa, F. S., Roig, A., & Sánchez-Monedero, M. A. (2010). Use of biochar as bulking agent for the composting of poultry manure: Effect on organic matter degradation and humification. *Bioresource Technology*, 101(4), 1239–1246. https://doi.org/10.1016/j.biortech.2009.09.024

Fischer, D., & Glaser, B. (2012). Synergisms between Compost and Biochar for Sustainable Soil Amelioration. *Management of Organic Waste*, 1, 167–198. https://doi.org/10.5772/31200

Firmino, M., V., & Trémier, A. (2023). Nitrogen Losses Mitigation by Supplementing Composting Mixture with Biochar: Research of the Ruling Parameters. *Waste and Biomass Valorization*, 1–13. https://doi.org/10.1007/s12649-023-02204-6

Fowler, D., Coyle, M., Skiba, U., Sutton, M. A., Cape, J. N., Reis, S., Sheppard, L. J., Jenkins, A., Grizzetti, B., Galloway, J. N., Vitousek, P., Leach, A., Bouwman, A. F., Butterbach-Bahl, K., Dentener, F., Stevenson, D., Amann, M., & Voss, M. (2013). The global nitrogen cycle in the twenty-first century. *Philosophical Transactions of the Royal Society B: Biological Sciences*, 368 (1621), 20130164. https://doi.org/10.1098/rstb.2013.0164

Fróna, D., Szenderák, J., & Harangi-Rákos, M. (2019). The Challenge of Feeding the World. *Sustainability*, 11(20), 5816. https://doi.org/10.3390/su11205816

Glaser, B., Balashov, E., Haumaier, L., Guggenberger, G., & Zech, W. (2000). Black carbon in density fractions of anthropogenic soils of the Brazilian Amazon region. *Organic Geochemistry,* 31(7-8), 669–678. https://doi.org/10.1016/S0146-6380(00)00044-9

Hagemann, N., Kammann, C. I., Schmidt, H. P., Kappler, A., & Behrens, S. (2017a). Nitrate capture and slow release in biochar amended compost and soil. *PloS one*, 12(2), e0171214. doi:10.1371/journal. pone.0171214

Hagemann, N., Joseph, S., Schmidt, H.-P., Kammann, C. I., Harter, J., Borch, T., Young, R. B., Varga, K., Taherymoosavi, S., Elliott, K. W., McKenna, A., Albu, M., Mayrhofer, C., Obst, M., Conte, P., Dieguez-Alonso, A., Orsetti, S., Subdiaga, E., Behrens, S., & Kappler, A. (2017b). Organic coating on biochar explains its nutrient retention and stimulation of soil fertility. *Nature Communications*, 8(1), 1089. https://doi.org/10.1038/s41467-017-01123-0

Hagemann, N., Subdiaga, E., Orsetti, S., La Rosa, J. M. de, Knicker, H., Schmidt, H.-P., Kappler, A., & Behrens, S. (2018). Effect of biochar amendment on compost organic matter composition following aerobic composting of manure. *The Science of the Total Environment,* 613-614, 20–29. https://doi.org/10.1016/j.scitotenv.2017.08.161

Haider, G., Steffens, D., Müller, C., & Kammann, C. I. (2016). Standard Extraction Methods May Underestimate Nitrate Stocks Captured by Field-Aged Biochar. *Journal of Environmental Quality*, 45(4), 1196–1204. https://doi.org/10.2134/jeq2015.10.0529

Haider, G., Joseph, S., Steffens, D., Müller, C., Taherymoosavi, S., Mitchell, D., & Kammann, C. I. (2020). Mineral nitrogen captured in field-aged biochar is plant-available. *Scientific Reports*, 10(1), 13816. https://doi.org/10.1038/s41598-020-70586-x

Harter, J., Guzman-Bustamante, I., Kuehfuss, S., Ruser, R., Well, R., Spott, O., Kappler, A., & Behrens, S. (2016). Gas entrapment and microbial N2O reduction reduce N2O emissions from a biochar-amended sandy clay loam soil. *Scientific Reports*, 6(1), 39574. https://doi.org/10.1038/srep39574

He, X., Chen, L., Han, L., Liu, N., Cui, R., Yin, H., & Huang, G. (2017). Evaluation of biochar powder on oxygen supply efficiency and global warming potential during mainstream large-scale aerobic composting. *Bioresource Technology*, 245, 309–317. https://doi.org/10.1016/j.biortech.2017.08.076

Hilscher, A., & Knicker, H. (2011). Degradation of grass-derived pyrogenic organic material, transport of the residues within a soil column and distribution in soil organic matter fractions during a 28 month microcosm experiment. *Organic Geochemistry*, 42(1), 42-54. https://doi.org/10.1016/j.orggeochem.2010.10.005

Hua, L., Chen, Y., Wu, W., & Ma, H. (2011). Microorganism communities and chemical characteristics in sludge-bamboo charcoal composting system. *Environmental Technology,* 32(5-6), 663–672. https://doi.org/10.1080/09593330.2010.510534

IPCC (2013). Climate change 2013: The physical science basis:Working Group I contribution to the fifth assessment report of the Intergovernmental Panel on climate change. *Cambridge University Press*. https://www.ipcc.ch/report/ar5/wg1/

Joseph, S., Kammann, C. I., Shepherd, J. G., Conte, P., Schmidt, H.-P., Hagemann, N., Rich, A. M., Marjo, C. E., Allen, J., Munroe, P., Mitchell, D. R. G., Donne, S., Spokas, K., & Graber, E. R. (2018). Microstructural and associated chemical changes during the composting of a high temperature biochar: Mechanisms for nitrate, phosphate and other nutrient retention and release. *The Science of the Total Environment*, 618, 1210–1223. https://doi.org/10.1016/j.scitotenv.2017.09.200

Jäckel, U., Thummes, K., & Kämpfer, P. (2005). Thermophilic methane production and oxidation in compost. *FEMS Microbiology Ecology*, 52(2), 175–184. https://doi.org/10.1016/j.femsec.2004.11.003

Jia, G., Shevliakova, E., Artaxo,P., De Noblet-Ducoudré, N., Houghton, R., House, J., Kitajima, K., Lennard, C., Popp, A., Sirin, A., Sukumar, R., Verchot, L. (2019). Land–climate interactions. In P. R. Shukla et al. (Ed.), *Climate Change and Land: an IPCC special report on climate change, desertification, land degradation, sustainable land management, food security, and greenhouse gas fluxes in terrestrial*, 131-248. https://doi.org/10.1017/9781009157988.004

Khan, N., Clark, I., Sánchez-Monedero, M. A., Shea, S., Meier, S., & Bolan, N. (2014). Maturity indices in co-composting of chicken manure and sawdust with biochar. *Bioresource Technology*, 168, 245–251. https://doi.org/10.1016/j.biortech.2014.02.123

Kammann, C. I., Schmidt, H.-P., Messerschmidt, N., Linsel, S., Steffens, D., Müller, C., Koyro, H.-W., Conte, P., & Joseph, S. (2015). Plant growth improvement mediated by nitrate capture in co-composted biochar. *Scientific Reports*, 5, 11080. https://doi.org/10.1038/srep11080

Kammann, C., Glaser, B., & Schmidt, H.-P. (2016). Combining biochar and organic amendments. In S.Shackley et al. (Ed.), Biochar in European Soils and Agriculture: *Science and Practice* 1 (pp.136–160). Routledge.

Knicker, H., Totsche, K. U., Almendros, G., & González-Vila, F. J. (2005). Condensation degree of burnt peat and plant residues and the reliability of solid-state VACP MAS 13C NMR spectra obtained from pyrogenic humic material. *Organic Geochemistry*, 36(10), 1359–1377. https://doi.org/10.1016/j.orggeochem.2005.06.006

Lasaridi, K., Protopapa, I., Kotsou, M., Pilidis, G., Manios, T., & Kyriacou, A. (2006). Quality assessment of composts in the Greek market: The need for standards and quality assurance. *Journal of Environmental Management*, 80(1), 58–65. https://doi.org/10.1016/j.jenvman.2005.08.011

Lehmann J.,& Joseph, S. (2009) Biochar for environmental management: an introduction. In: Lehmann, J.,& Joseph, S. (Ed.), *Biochar for environmental management: science and technology* (pp.1-12). Earthscan.

Lehmann, J., Cowie, A., Masiello, C. A., Kammann, C., Woolf, D., Amonette, J. E., Cayuela, M. L., Camps-Arbestain, M., & Whitman, T. (2021). Biochar in climate change mitigation. *Nature Geoscience*, 14(12), 883–892. https://doi.org/10.1038/s41561-021-00852-8

Le Leuch, L. M., & Bandosz, T. J. (2007). The role of water and surface acidity on the reactive adsorption of ammonia on modified activated carbons. *Carbon*, 45(3), 568–578. https://doi.org/10.1016/j.carbon.2006.10.016

Li, Y., Yu, S., Strong, J., & Wang, H. (2012). Are the biogeochemical cycles of carbon, nitrogen, sulfur, and phosphorus driven by the "FeIII–FeII redox wheel" in dynamic redox environments? *Journal of Soils and Sediments*, 12(5), 683–693. https://doi.org/10.1007/s11368-012-0507-z

Li, R., Wang, Q., Zhang, Z., Zhang, G., Li, Z., Wang, L., & Zheng, J. (2015). Nutrient transformation during aerobic composting of pig manure with biochar prepared at different temperatures. *Environmental Technology,* 36(5-8), 815–826. https://doi.org/10.1080/09593330.2014.963692

Li, S., Song, L., Jin, Y., Liu, S., Shen, Q., & Zou, J. (2016). Linking N2O emission from biochar-amended composting process to the abundance of denitrify (nirK and nosZ) bacteria community. *AMB Express*, 6(1), 37. https://doi.org/10.1186/s13568-016-0208-x

Liu, N., Zhou, J., Han, L., Ma, S., Sun, X., & Huang, G. (2017). Role and multi-scale characterization of bamboo biochar during poultry manure aerobic composting. *BioresourceTechnology*,241,190–199. https://doi.org/10.1016/j.biortech.2017.03.144

Liu, Q., Zhang, Y., Liu, B., Amonette, J. E., Lin, Z., Liu, G., Ambus, P., & Xie, Z. (2018). How does biochar influence soil N cycle? A meta-analysis. *Plant and soil*, 426(1-2), 211–225. https://doi.org/10.1007/s11104-018-3619-4

Loganathan, P., Vigneswaran, S., & Kandasamy, J. (2013). Enhanced removal of nitrate from water using surface modification of adsorbents—a review. *Journal of Environmental Management*, 131, 363–374. https://doi.org/10.1016/j.jenvman.2013.09.034

López-Cano, I., Roig, A., Cayuela, M. L., Alburquerque, J. A., & Sánchez-Monedero, M. A. (2016). Biochar improves N cycling during composting of olive mill wastes and sheep manure. *Waste Management*, 49, 553–559. https://doi.org/10.1016/j.wasman.2015.12.031

Maheshwari, D. K. (2014). Composting for sustainable agriculture (Vol. 3). *Springer International*. https://doi.org/10.1007/978-3-319-08004-8

FAO (2008). *Guide to laboratory establishment for plant nutrient analysis (FAO fertilizer and plant nutrition).* Bulletin No. TC/M/I0131E/1/07.08/1100). Food and Agriculture Organization of the United Nations.

Nguyen, M. K., Lin, C., Hoang, H. G., Sanderson, P., Dang, B. T., Bui, X. T., Nguyen, N. S. H., Vo, D.-V. N., & Tran, H. T. (2022). Evaluate the role of biochar during the organic waste composting process: A critical review. *Chemosphere*, 299, 134488. https://doi.org/10.1016/j.chemosphere.2022.134488

Prost, K., Borchard, N., Siemens, J., Kautz, T., Séquaris, J.-M., Möller, A., & Amelung, W. (2013). Biochar affected by composting with farmyard manure. *Journal of Environmental Quality*, 42(1), 164–172. https://doi.org/10.2134/jeq2012.0064

Román, P., Martinez, M. M., & Pantoja, A. (2015). Farmers America, handbook experiences in Latin America. Food and Agriculture Organization of the United Nations

Rynk, R., van de Kamp, M., Willson, G. B., Singley, M. E., Richard, T. L., Kolega, J. J., Gouin, F., Laliberty, L., Kay, D., Murphy, D., Hoitink, H., & Brinton, W. F. (1992). On-farm composting handbook. *Northeast Regional Agricultural Engineering Service,* 152, 14853-5701. https://ecommons.cornell.edu/handle/1813/67142

Sánchez, A., Artola, A., Font, X., Gea, T., Barrena, R., Gabriel, D., Sánchez-Monedero, M. Á., Roig, A., Cayuela, M. L., & Mondini, C. (2015). Greenhouse gas emissions from organic waste composting. *Environmental Chemistry Letters*, 13(3), 223–238. https://doi.org/10.1007/s10311-015-0507-5

Sánchez-García, M., Alburquerque, J. A., Sánchez-Monedero, M. A., Roig, A., & Cayuela, M. L. (2015). Biochar accelerates organic matter degradation and enhances N mineralisation during composting of poultry manure without a relevant impact on gas emissions. *Bioresource Technology,*192,272–279. https://doi.org/10.1016/j.biortech.2015.05.003

Sánchez-Monedero, M. A., Roig, A., Paredes, C., & Bernal, M. P. (2001). Nitrogen transformation during organic waste composting by the Rutgers system and its effects on pH, EC and maturity of the composting mixtures. *Bioresource Technology*, 78(3), 301–308. https://doi.org/10.1016/S0960-8524(01)00031-1

Sánchez-Monedero, M. A., Cayuela, M. L., Roig, A., Jindo, K., Mondini, C., & Bolan, N. (2018). Role of biochar as an additive in organic waste composting. *Bioresource Technology*, 247, 1155–1164. https://doi.org/10.1016/j.biortech.2017.09.193

Schaefer, Y. (2020). Impact of biochar on nutrient dynamics during composting of humanure, cattle manure and other organic materials – A Case study from South Ethiopia [Master's thesis, University of Bonn].

Schmidt, H. P., Kammann, C., Hagemann, N., Leifeld, J., Bucheli, T.D., Sánchez-Monedero, M. A., & Cayuela, M.L. (2021). Biochar in agriculture- A systematic review of 26 global meta-analyses. *GCB Bioenergy*, 13 (11), 17081730. https://doi.org/10.1111/gcbb.12889

Schmid, C. A. O., Reichel, R., Schröder, P., Brüggemann, N., & Schloter, M. (2020). 52 years of ecological restoration following a major disturbance by opencast lignite mining does not reassemble microbiome structures of the original arable soils. *The Science of the Total Environment,* 745, 140955. https://doi.org/10.1016/j.scitotenv.2020.140955

Sonoki, T., Furukawa, T., Jindo, K., Suto, K., Aoyama, M., & Sánchez-Monedero, M. Á. (2013). Influence of biochar addition on methane metabolism during thermophilic phase of composting. *Journal of Basic Microbiology*, 53(7), 617–621. https://doi.org/10.1002/jobm.201200096

Steiner, C., Das, K. C., Melear, N., & Lakly, D. (2010). Reducing nitrogen loss during poultry litter composting using biochar. *Journal of Environmental Quality*, 39(4), 1236–1242. https://doi.org/10.2134/jeq2009.0337

Sun, D., Lan, Y., Xu, E. G., Meng, J., & Chen, W. (2016). Biochar as a novel niche for culturing microbial communities in composting. *Waste Management*, 54, 93–100. https://doi.org/10.1016/j.wasman.2016.05.004

VDLUFA (2008). VDLUFA—Methodenbuch Band II.2. *Die Untersuchung von Sekundärrohstoffdüngern, Kultursubstraten und Bödenhilfsstoffen: Bestimmung von Phosphor und Kalium im Calcium-Acetat-Lactat-Auszug.* VDLUFA.

VDLUFA (2014). VDLUFA—Methodenbuch Band II.2. *Die Untersuchung von Sekundärrohstoffdüngern, Kultursubstraten und Bödenhilfsstoffen: Bestimmung des wesentlichen Gehaltes an verfügbarem Stickstoff (Ammonium und Nitrat): CaCl2-Auszug*. VDLUFA.

Wang, Y., Lin, Y., Chiu, P. C., Imhoff, P. T., & Guo, M. (2015). Phosphorus release behaviors of poultry litter biochar as a soil amendment. *The Science of the Total Environment*, 512-513, 454–463. https://doi.org/10.1016/j.scitotenv.2015.01.093

Wang, Q., Awasthi, M. K., Ren, X., Zhao, J., Li, R., Wang, Z., Wang, M., Chen, H., & Zhang, Z. (2018). Combining biochar, zeolite and wood vinegar for composting of pig manure: The effect on greenhouse gas emission and nitrogen conservation. *Waste Management,* 74, 221–230. https://doi.org/10.1016/j.wasman.2018.01.015

Wang, Y., Villamil, M. B., Davidson, P. C., & Akdeniz, N. (2019). A quantitative understanding of the role of co-composted biochar in plant growth using meta-analysis. *The Science of the Total Environment*, 685, 741–752. https://doi.org/10.1016/j.scitotenv.2019.06.244

Wang, H., Lu, Y., Xu, J., Liu, X., & Sheng, L. (2021). Effects of additives on nitrogen transformation and greenhouse gases emission of co-composting for deer manure and corn straw. *Environmental Science and Pollution Research International,* 28(10), 13000–13020. https://doi.org/10.1007/s11356-020-11302-0

Wang, L., Olsen, M. N., Moni, C., Dieguez-Alonso, A., La Rosa, J. M. de, Stenrød, M., Liu, X., & Mao, L. (2022). Comparison of properties of biochar produced from different types of lignocellulosic biomass by slow pyrolysis at 600 °C. *Applications in Energy and Combustion Science,* 12, 100090. https://doi.org/10.1016/j.jaecs.2022.100090

Wiedner, K., Fischer, D., Walther, S., Criscuoli, I., Favilli, F., Nelle, O., & Glaser, B. (2015). Acceleration of Biochar Surface Oxidation during Composting? *Journal of Agricultural and Food Chemistry,* 63(15), 3830–3837. https://doi.org/10.1021/acs.jafc.5b00846

Yin, Y., Yang, C., Li, M., Zheng, Y., Ge, C., Gu, J., Li, H., Duan, M., Wang, X., & Chen, R. (2021). Research progress and prospects for using biochar to mitigate greenhouse gas emissions during composting: A review. *The Science of the Total Environment*, 798, 149294. https://doi.org/10.1016/j.scitotenv.2021.149294

Zhang, L., & Sun, X. (2014). Changes in physical, chemical, and microbiological properties during the two-stage co-composting of green waste with spent mushroom compost and biochar. *Bioresource Technology,* 171, 274–284. https://doi.org/10.1016/j.biortech.2014.08.079

Zucconi, F. (1981). Evaluating toxicity of immature compost. *BioCycle*, 0, 54–57. https://cir.nii.ac.jp/crid/1571135650109373312

Appendices

Appendix A: Experimental set up

Figure A.1 Collection of fresh horse manure on July 4, 2022 at the Stütgerhof horse ranch (Langerwehe)

Figure A.2 Collection of fresh and chopped scraps on July 5, 2022 at Burgmühle (Kerpen)

Figure A.3 Mixing vegetable scraps, horse manure and wheat straw with garden forks on July 6, 2022 at Forschungszentrum Jülich

Figure A.4 Wooden compost boxes before filling (left) and after a few days of composting (right).

Figure A.5 Compost boxes with compost fleece, straw insulation and pond liner.

Figure A.6 Four static PVC tubes for periodic gas sampling with a syringe (right).

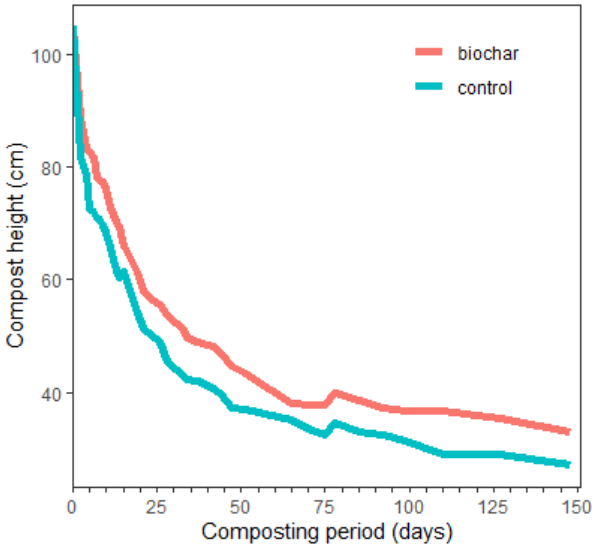

Figure A.7 Development of the compost height during 148 days of composting.

Appendix B: Additional Information on biochar

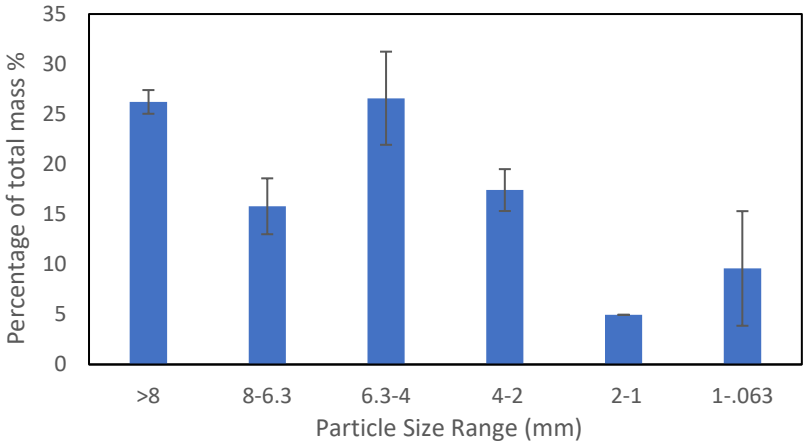

Figure A.8 Particle size distribution of woody biochar using the dry sieving method

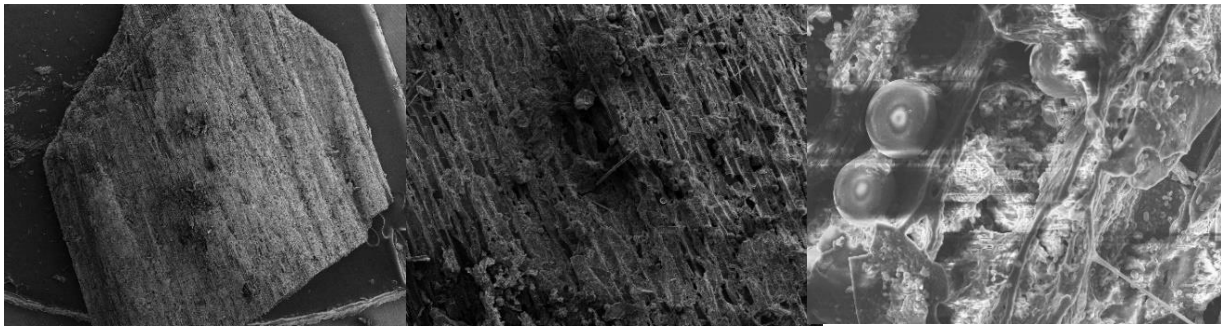

Figure A.9 *SEM-EDX images of the biochar after 148 days of co-composting.*

Table A.1 *Physical and chemical properties of the biochar used in this study. Values were obtained from Eurofins Umwelt Ost GmbH according to EBC regulations.*

		biochar as-delivered condition	water-free
Ash content (550°C) (%)	-	3.2	5.1
Ash content (815°C) (%)	-	2.2	3.6
TC (%)	-	56.5	90.3
O_2	-	2.5	4.1
H:C	-	0.17	0.17
Salinity (g kg^{-1})	-	3.17	
Determination from microwave pressure digestion according to DIN 22022-1: 2014-07			
Cu (mg kg^{-1})	-	-	4
Ni (mg kg^{-1})	-	-	10
Zn (mg kg^{-1})	-	-	50
Cr (mg kg^{-1})	-	-	12
B (mg kg^{-1})	-	-	53
Mn (mg kg^{-1})	-	-	535
Ag (mg kg^{-1})	-	-	< 5
Determination from pressure digestion according to DIN EN 13805: 2014-12			
As (mg kg^{-1} 88% dw)	0.14	-	-
Pb (mg kg^{-1} 88% dw)	0.8	-	-
Cd (mg kg^{-1} 88% dw)	0.03	-	-
Hg (mg kg^{-1} 88% dw)	0.0032	-	-
Elements in the ash 550°C DIN 51729-11: 1998-11			
Fe_2O_3 (g kg^{-1})	-	-	0.6
Na_2O (g kg^{-1})	-	-	0.1
SiO_2 (g kg^{-1})	-	-	7.3

Appendix C: Additional information on measurements

Table A.2 *Schedule of compost measurements: Temperature (Temp), gas chromatography (GC) interval, compost sampling for nutrient analysis and moisture content, turning and watering of piles, germination index (GI) test, and other adjustments.*

Day	Temp	GC interval	Compost sampling	Turning	watering	GI	Other adjustments
							collection of HM 1
							collection of VS
0	x			x			collection of HM 2
1	x	5-10-15-20	x				
2	x	5-10-15-20					
3	x						
4	x						
5	x	5-10-15-20					
6	x						
7	x	5-10-15-20					
8	x		x				
9	x	5-10-15-20					
10	x						
11	x						
12	x						
13	x	5-10-15-20					
14	x	5-10-15-20					
15	x		x	x			
16	x	5-10-15-20					
17	x						
18	x						
19	x	5-10-15-20					
20	x						
21	x	5-10-15-20					
22	x		x				
23	x	5-10-15-20					
24	x						
25	x						
26	x	5-10-15-20					
27	x						
28	x	5-10-15-20					
29	x		x				
30	x	10-20-30-40					
31	x						
32	x						
33	x						
34	x				1l/box		insulation
35	x	10-20-30-40					
36	x		x				
37	x	10-20-30-40			3l/box		

38	x						
40	x	10-20-30-40					
41				x	5l/box		
42		10-20-30-40					
43			x				
44	x	10-20-30-40					
47	x	10-20-30-40					
49	x	10-20-30-40					
50			x				
51	x	15-30-45-60					
54	x	15-30-45-60					
55							
56	x	15-30-45-60					
57			x				
58	x	15-30-45-60					
61	x	20-40-60-80					
63	x	20-40-60-80					
64			x				
65	x	20-40-60-80					
68	x	20-40-60-80					
71	x	20-40-60-80	x				
75	x	20-40-60-80					pond liner
77			x	x			
78	x				2l/box		
79		20-40-60-80					
84			x				
85	x	25-50-75-100					
92	x	30-60-90-120					
96			x			x	
99	x	30-60-90-120					
104			x			x	
108				x			
110	x	35-70-105-140					
126			x			x	
127	x	40-80-120-160					
139			x			x	
148	x	45-90-135-180	x				

Appendix D: Critical addendum on the methods

The methods used to monitor the parameters of the experiment were able to adequately reflect the temporal dynamics of the compost. However, the results recorded are not always uniform. Particularly remarkable in this experiment was the large variability within replicates which is a common issue in field experiments and might have arise due to the substrate composition, microbial activity or environmental conditions.

Often no significant differences between treatments could be found, so the derived trends were discussed. Differences were also found within the boxes due to the large heterogeneity of the compost substrate. The gas measurements in particular showed very large variations. It should be emphasized that the compost experiment was conducted outdoors and was therefore exposed to various environmental influences. Although all the boxes had the standardized conditions (same amount of substrate, covered with fleece, no direct contact with the soil, insulation of the outside with straw), it is possible that micro-effects due to external factors such as wind or radiation still occurred. In addition, only three replicates per treatment could be constructed, making it difficult to perform a comprehensive representative statistic analysis, to identify statistical outliers and obtain robust results. The experimental set-up was originally designed for four replicates per treatment, but the amount of raw material supplied was only sufficient to achieve the required filling level of six boxes.

Measurement errors in the laboratory can in principle be excluded by precise laboratory work. However, the stepwise extraction of retained NO_3^- from the bc revealed an error which is not discussed further in the results. On day 8, a concentration of highly bound NO_3^-–N was measured in replicate B, but this was not consistent with the other replicates or with subsequent measurements.

Some parameters could not be sufficiently sampled due to technical problems and the availability of the necessary equipment. An FTIR analyzer (infrared spectroscopy) was also used to measure CO_2, CH_4, N_2O and NH_3 in parallel with the gas chromatography measurements. However, due to condensation and technical problems at the beginning of the experiment and the resulting interruption of the measurement series, these data could not be used. It was also not possible to perform the Dräger tube method continuously. The NH_3 data would have provided interesting conclusions on N losses by NH_3 volatilization at high pH.

The evaluation of the SEM-EDX images could not be completed within the timeframe of the Master's thesis and is therefore only included in the appendix (Appendix: Figure A.8), but not discussed further. The images could offer valuable information about the co-composted bc, the microstructure and nutrient adsorption. Despite these difficulties, the composting experiment provides important and relevant results.